HOKKAIDO UNIVERSITY

Title	On the extraordinary snow on the sea ice off East Antarctica in late winter, 2012
Author(s)	Toyota, Takenobu; Massom, Robert; Lecomte, Olivier et al.
Citation	Deep Sea Research Part II Topical Studies in Oceanography, 131, 53-67 https://doi.org/10.1016/j.dsr2.2016.02.003
Issue Date	2016-02-09
Doc URL	https://hdl.handle.net/2115/68311
Rights	©2016, Elsevier. This manuscript version is made available under the CC-BY-NC-ND 4.0 license http://creativecommons.org/licenses/by-nc-nd/4.0/
Rights(URL)	https://creativecommons.org/licenses/by-nc-nd/4.0/
Type	journal article
File Information	sipex2_snow_man_rev2 02 -.pdf

Hokkaido University Collection of Scholarly and Academic Papers : HUSCAP

Title:

On the extraordinary snow on the sea ice off East Antarctica in late winter, 2012

Authors:

Takenobu Toyota[1], Robert Massom[2,3], Olivier Lecomte[4], Daiki Nomura[1], Petra Heil[2,3], Takeshi Tamura[3,5,6], Alexander D. Fraser[1,3]

Submitted to Deep-Sea Research II

Affiliation

1*: Institute of Low Temperature Science, Hokkaido University N19W8, Kita-ku, Sapporo, 060-0819, Japan (toyota@lowtem.hokudai.ac.jp)

*Corresponding author

Tel: +81-11-706-7431 Fax: +81-11-706-7142

2: Department of the Environment, Australian Antarctic Division, 203 Channel Highway, Kingston, Tasmania 7050, Australia

3: Antarctic Climate & Ecosystems Cooperative Research Centre, University of Tasmania, Private Bag 80, Hobart, Tasmania 7001, Australia

4: Université Catholique de Louvain, Louvain-la-Neuve, Belgium

5: National Institute of Polar Research, Tokyo, Japan

6: SOKENDAI (The Graduate University for Advanced Studies), Tachikawa, Tokyo 190-8518, Japan

Abstract

In late winter-early spring 2012, the second Sea Ice Physics and Ecosystems Experiment (SIPEX II) was conducted off Wilkes Land, East Antarctica, onboard *R/V Aurora Australis*. The sea-ice conditions were characterized by significantly thick first-year ice and snow, trapping the ship for about 10 days in the near coastal region. The deep snow cover was particularly remarkable, in that its average value of 0.45 m was almost three times that observed between 1992 and 2007 in the region. To reveal factors responsible, we used in situ observations and ERA-Interim reanalysis (1990 – 2012) to examine the relative contribution of the different components of the local-regional snow mass balance equation i.e., snow accumulation on sea ice, precipitation minus evaporation (*P-E*), and loss by i) snow-ice formation and ii) entering into leads due to drifting snow. Results show no evidence for significantly high *P-E* in the winter of 2012. Ice core analysis has shown that although the snow-ice layer was relatively thin, indicating less transformation from snow to snow-ice in 2012 as compared to measurements from 2007, the difference was not enough to explain the extraordinarily deep snow. Based on these results, we deduce that lower loss of snow into leads was probably responsible for the extraordinary snow in 2012. Statistical analysis and satellite images suggest that the reduction in loss of snow into leads is attributed to rough ice surface associated with active deformation processes and larger floe size due to sea-ice expansion. This highlights the importance of snow-sea ice interaction in determining the mean snow depth on Antarctic sea ice.

Keyword: Antarctic snow on sea ice, Snow accumulation around the Antarctic, Snow-ice formation, loss of snow into leads, ERA-Interim

Regional index term: East Antarctica

1. Introduction

Snow on sea ice is a very important factor in shaping the polar climate and ecosystems. While sea ice plays a significant role in the exchange of energy between the ocean and the atmosphere that determines the polar climate (Serreze et al., 2007), snow modifies the properties of sea ice in several ways. Thermodynamically, snow significantly enhances the insulating effect of sea ice through its higher albedo, its lower thermal conductivity, and its lower volumetric specific heat capacity compared to sea ice (Ishii and Toyota, 2012; Ledley, 1991; Sturm and Massom, 2010). On the other hand, snow contributes to the growth of sea ice through its transformation to snow ice when an excessive snow load depresses the snow/ice interface below the sea level and the resultant water-saturated snow refreezes (Jeffries et al., 2001; Maksym and Jeffries, 2000). Furthermore, it has been revealed that snow plays an important role in the biogeochemical system as a reservoir and carrier of chemical components precipitated from the atmosphere (e.g. Kanna et al., 2014; Nomura et al., 2010) and as a control on the amount of light available for growth of algae within the sea ice and underlying water column (Eicken, 1992).

The strength of these effects depends on the snow depth relative to sea-ice thickness, and it is shown from numerical modeling studies that the sensitivity of snow depth to ice growth or decay is high in Antarctica where relatively thin sea ice predominates compared with the Arctic (Fichefet and Morales-Maqueda, 1999). Indeed, whereas snow-ice formation is uncommon in the Arctic sea ice, it occurs over large areas and snow ice accounts for an estimated 10-40% of total Antarctic sea-ice thickness (Jeffries et al., 1994, 1997). This contribution is shown to be particularly high off Wilkes Land, East Antarctica, where sea ice is relatively thin and snow accumulation rates are

relatively high compared with other Antarctic areas (Maksym and Markus, 2008). Therefore, to interpret the long-term trend of the sea-ice characteristics in this area, it is important to know the interannual variability of snow properties including the accumulation rates, which are presumed to control snow depth.

Unfortunately, this is a major challenge, due to a lack of long-term observations and the following factors. While satellite passive microwave remote sensing provides large-scale estimates of snow-depth distribution over the entire Antarctic sea-ice zone (Markus and Cavalieri, 1998; Powell et al., 2005), comparison of large-scale snow-depth distribution with *in situ* data obtained off East Antarctica indicates significant underestimation of actual snow thickness in regions of rough ice (Worby et al., 2008) i.e., independent information on ice-surface roughness is required to improve snow-thickness retrieval accuracy from the satellite data (Markus et al., 2011). Other work has attributed an apparent discrepancy between snow accumulation and observed snow depth to “loss” due to snow ice formation and wind transport into leads between ice floes (Leonard and Maksym, 2011). An apparent discrepancy exists between the fraction of snow ice to total ice thickness off East Antarctica from satellite-derived snow depth and meteorological reanalysis snowfall products (Maksym and Markus, 2008) compared to *in situ* observations (Worby et al., 1998) i.e., ~30% versus ~13%, respectively. Although snow loss into leads is considered to be significant over the entire Southern Ocean (Eicken et al., 1994; Leonard and Maksym, 2011), observational data have not been collected off East Antarctica (to the authors’ knowledge). Therefore, the fate of snow accumulated on sea ice in this region is still an open question.

According to the previous observations off East Antarctica conducted intermittently for winters between 1992 and 2007, mean snow depth was about 0.15 m with only a

small interannual variability (Toyota et al., 2011). However, during SIPEX II, conducted in the same region in late winter 2012, it was found that the mean snow depth amounted to 0.45±0.26 (standard deviation, hereafter referred to as sd) m, i.e., it was about three times thicker than the previous results. This indicates the possibility of a large interannual variability in snow depth in this area, and that the apparent small variability obtained prior to 2012 might be due to sampling bias. To understand the real interannual variability in snow depth and its controlling factors off East Antarctica, more complete data analysis using both meteorological dataset and field data is required.

The aim of this paper is to clarify what caused significantly deep snow depth off East Antarctica in 2012 compared with previous observations, with a view to estimating the snow mass balance on the wintertime sea-ice cover in the region and to improve understanding of snow-sea ice interaction processes and how they vary. To do so, we examine the interannual variability of snow accumulation rates on sea ice in winter for the whole Antarctic region using meteorological reanalysis (ERA-Interim) for 1990 to 2012, to enable direct comparison with previous observations. Snow accumulation rates are estimated by calculating precipitation minus evaporation (*P*-*E*) from the moisture budget. We analyzed the whole Antarctic sea-ice area in order to i) accommodate the effect of sea-ice drift/motion on snow accumulation patterns, and ii) resolve any strong interannual variability in precipitation on a hemispheric scale. From the field observations, we estimate the snow-depth distribution and the thickness of snow ice from the ice cores, focusing on comparing 2007 and 2012. Though the data are rather limited, this analysis allows us to quantitatively estimate the fate of snow on sea ice in this region.

2. Data

2-1. Field measurements

The field data used in this study are from 5 ice stations conducted from the *R/V Aurora Australis* in the seasonal sea-ice zone off Wilkes Land, East Antarctica between September 23 and November 11, 2012. This dataset is composed of four kinds of measurements: 1) snow, sea-ice thickness, and freeboard profiles (drill hole measurements) at 1 m intervals along 11 transect lines (each 100 m long) in total; 2) detailed vertical profiles of snow properties at 18 snow pits on 5 floes; 3) diurnal observations of temperature profiles and snow properties; and 4) vertical profiles of sea-ice properties derived from the ice-core samples.

The snow pit measurements included detailed assessment of snow stratigraphy, snow type classification (based upon the *International Classification for Seasonal Snow on the Ground* [Fierz et al., 2009]), and vertical profiles of temperature, grain size, density and salinity. Snow density and salinity were measured using a standard 3 cm-high snow sampler with a volume of 100 cm^3. To avoid contamination by seawater, snow-pit observations were completed before the sea ice was penetrated by drilling.

Diurnal observations included measurements of vertical temperature profiles, salinity and density within the basal layer, and were conducted every two hours at four ice stations on September 27-28, October 3-4, October 6-8, and October 13-14 when the ship remained alongside a floe for longer than one day. The observation sites were located on relatively flat areas a few tens of metres away from both the transect line and the ship to avoid any interference. Diurnal observations were intended to examine the temporal evolution of temperature profiles on a diurnal time scale and its effect on the snow metamorphism. The results are used to discuss the localized feature of

147 precipitation (section 5) and the effect of snow wetness on vertical heat flux through
148 snow (Lecomte and Toyota, *DSR2* [this volume]).

149 In addition, and to estimate the contribution of snow ice, we analyzed 32 sea ice
150 cores from 14 ice stations in 2007 and 7 from 6 ice stations in 2012. The relative lack of
151 ice stations in 2012 was indicative of the difficult conditions encountered in that year.
152 However, we regard the data as representative to some extent because we selected
153 relatively flat areas for the sampling locations to avoid local scale variability. For each
154 sample, we made vertical thin sections in the freezer laboratory aboard the *R/V Aurora*
155 *Australis* to see the crystal alignments. After sectioning the cores vertically into
156 segments a few to 10 cm thick and melting them, we measured $\delta^{18}O$ and salinity to see
157 the vertical profiles. The $\delta^{18}O$ was determined with a DELTA plus mass spectrometer at
158 Hokkaido University and a SIRA-Isoprep water-equilibration mass spectrometer at
159 University of Tasmania with the analytical precisions of 0.02‰ and <0.04‰,
160 respectively. Salinity was measured with a conductivity sensor (Cond 330i, WTW,
161 Germany) with a nominal accuracy of 0.1.

162

163 **2-2. Meteorological reanalysis dataset**

164 We used the 6-hourly ERA-Interim reanalysis to calculate net precipitation
165 (precipitation minus sublimation/evaporation) from 1990 to 2012. With this dataset, we
166 calculated net precipitation from the atmospheric moisture budget equation (Bromwich,
167 1988; Cullather et al., 1998; Yamazaki, 1992). The horizontal resolution of the dataset is
168 1.5^{o} by 1.5^{o} and the analysis area is the whole Antarctic region south of 60^{o} S, most of
169 which is covered with sea ice in winter (Fig. 1). The whole Antarctic region is further
170 divided into five sectors to examine the regional characteristics. Figure 1a shows the

divisions of the Antarctic region with our observation area in 2007 and 2012 i.e., 63.0^{o} to 66.0^{o} S and 115.5^{o} to 127.5^{o} E (1.97 x 10^5 km^2). To calculate the vertically-integrated moisture flux and precipitable water, we used air pressure, horizontal wind components, air temperature, and dew point temperature at the surface, and relative humidity, air temperature, horizontal wind components at 10 standard levels (950, 900, 850, 800, 700, 600, 500, 400, 300, 200 hPa). Since specific humidity is concentrated below 700 hPa and is essentially zero above 200 hPa and throughout the year, the data above 200 hPa were neglected. Although a snowfall product is provided by the ERA-Interim dataset, we took this traditional method following Cullather et al. (1998). This is because i) true snow-accumulation rates on sea ice are determined not only by snowfall amount but also by *P-E*, and accurate estimation of evaporation from the snow surface is difficult; and ii) the estimation of *P-E* calculated based on the moisture budget equation seems more consistent from the standpoint of moisture conservation if winds and specific humidity are properly reproduced.

3. Analytical method

3-1. Estimation of snow accumulation

For the Antarctic continent, the surface snow accumulation and precipitation rates (*B* and *P* respectively) are related by the following equation (Bromwich, 1988; Cullather et al., 1998):

$$\overline{\langle B \rangle} = \overline{\langle P \rangle} - \overline{\langle E \rangle} - \overline{\langle D \rangle} - \overline{\langle M \rangle}, \quad (1)$$

where *E* is the net sublimation rate (i.e., sublimation minus deposition of hoarfrost); *D* is the deposition rate of snow by drifting; *M* is the divergence of melt water runoff; and angled brackets and overbar represent areal and time averages, respectively. For the

Antarctic continent as a whole, the contribution of D and M in Eq.1 is small relative to P and E (Bromwich, 1988). Therefore, for a first-order discussion, the snow accumulation is determined by net precipitation (P minus E).

In the case of snow on sea ice, there are two additional terms: rate of conversion of snow into snow-ice (I) and rate of loss of snow into open water leads and cracks (L) (Leonard and Maksym, 2011). Wind-blown snow redistribution on sea ice is considered to have no essential effect on snow-mass balance for annual averages on a large horizontal scale (Bromwich, 1988, 1990). Therefore the snow-mass balance on sea ice is represented by the following equation:

$$\overline{\langle B \rangle} = \overline{\langle P \rangle} - \overline{\langle E \rangle} - \overline{\langle I \rangle} - \overline{\langle L \rangle} \quad (2)$$

In this study, we examine the budget of snow on sea ice on a seasonal time scale. Therefore, $\overline{\langle B \rangle}$ corresponds to the mean snow depth observed during the SIPEX II. The net precipitation, $\overline{\langle P \rangle} - \overline{\langle E \rangle}$, is estimated from the following moisture budget equation using the ERA-Interim reanalysis dataset:

$$P - E = -\frac{\partial PW}{\partial t} - \nabla \cdot \frac{1}{g} \int_{pt}^{ps} q\vec{V}\, dp, \quad (3)$$

where PW is precipitable water; g is the gravitational acceleration; p is pressure in hPa; p_s and p_t are the pressure in hPa at the surface and the top of atmosphere, respectively; $\vec{V}$ is the horizontal wind vector; and q is specific humidity in g kg^{-1} at each level and calculated from the following equation:

$$q = \frac{0.622\, e}{p - 0.378\, e} \times 1000 \quad (4)$$

where e is water vapour pressure in hPa. This is calculated from relative humidity and air temperature using the Tetens formula, and PW is then obtained by vertically integrating q from the surface (p_s) to 200 hPa level (p_t), as follows:

$$PW = \frac{1}{g} \int_{pt}^{ps} q\, dp \quad (5)$$

Since q is essentially zero above 200 hPa, we set p_t to 200 hPa. Eq.3 means that P and E are sink and source terms of PW, respectively. Assuming that Eq.3 can be applied on a daily time scale, we calculate P-E on a daily basis by substituting the daily mean values of q and $q\vec{V}$ into Eq.3. Next, to estimate the total net precipitation (= $\overline{\langle P \rangle} - \overline{\langle E \rangle}$ in Eq.2), the daily P-E data were summed for each winter.

In this analysis, the integration period is important because it directly affects the total snow accumulation. Here, we set it from May 1 to September 30 for every year on the basis that advancing sea ice usually starts to cover the observation area at the beginning of May (Fig.2; see also Massom et al., 2013). Although there are some interannual variations in the growth phase of sea-ice area, we decided to fix the integration period because it is quite difficult to determine the beginning date of snow accumulation on the specific sea ice in the observation area and to predict the fate of that floe.

In calculating P-E, Cullather et al. (1998) corrected the divergent wind so as to satisfy the conservation of columnar dry-air mass, following Trenberth (1991). However, in this study we refrained from this correction for the following reasons. While the correction method of Trenberth (1991) is based on the assumption that the wind-related error occurs uniformly through the full depth of the atmosphere, the influential layer from the standpoint of the moisture budget is only near the surface. Therefore, this method may not necessarily be appropriate for the moisture budget equation. In addition, and according to Cullather et al. (1998), the mass correction only works effectively in the coastal regions such as the Antarctic Peninsula, and the difference made by applying this correction to the net precipitation rate is relatively small over the sea-ice area i.e., (-40 to 0 kg m^{-2} yr^{-1}).

Values for term $\overline{\langle I \rangle}$ in Eq.2 are estimated from the ice-core samples collected during the cruises in 2007 and 2012, through analysis of vertical profiles of crystallography in thin section and $\delta^{18}O$ for melted samples i.e., snow ice layer is granular with a negative $\delta^{18}O$. The criterion for $\delta^{18}O$ is based on the observational results of the seawater $\delta^{18}O$ just below the sea ice (-0.41‰ to -0.23‰), taking into account the fractionation during the freezing (Toyota et al., 2013). This criterion is the same as that used for Antarctic sea ice by Jeffries et al. (1997) and for Sea of Okhotsk ice by Toyota et al. (2004). To estimate the thickness of snow that is converted into snow-ice (h_s), we introduce a compression parameter β describing how snow is compressed in the snow-ice formation process, following Leppäranta and Kosloff (2000):

$$h_s = \beta \cdot h_{si}, \qquad (6)$$

where h_{si} is the analyzed snow-ice thickness. Based on the observations at Lake Pääjärvi in southern Finland, Leppäranta and Kosloff (2000) estimated β to be 1.5. In this study, we use the same value because the process is considered to be similar. Then, the amount of loss of snow into leads and cracks, $\overline{\langle L \rangle}$, is obtained as a residual of Eq. 2.

3-2. Validation of the method

While net precipitation rate obtained from the moisture budget equation has been validated over the ice sheet (Bromwich et al., 1995; Yamazaki, 1992), validation is more difficult over the sea ice due to a lack of monitoring sites for snow accumulation. In this study, we validate this method by checking to what extent the ERA-Interim dataset reproduced the ship-based data obtained in 2012, and by comparing the calculated annual mean *P-E* with past studies.

Figure 3 shows the time series of sea level pressure (SLP), air temperature (SAT), vapour pressure, wind components, and specific humidity recorded every 10 minutes onboard the ship, together with 6-hourly ERA-Interim surface data at the grids closest to the ship positions being plotted. Specific humidity in g kg^{-1} was calculated from Eq.4. Since the observation period of SLP was limited to October 9 to 29, q is also limited to the same period. It is shown in Fig.3 that, as a whole, all the elements of the ERA-Interim reproduced the observations well, except for some discrepancies on a small scale. When we compare the daily mean data from these two datasets, the correlation coefficients are 0.97 (+1.4 and 2.6 hPa) for SLP; 0.91 (+0.5 and 1.8 ^{o}C) for SAT; 0.87 (+0.6 and 3.1 m s^{-1}) for the zonal component of wind; 0.89 (-0.4 and 1.9 m s^{-1}) for the meridional component of wind; 0.88 (0.0 and 0.4 hPa) for vapour pressure; and 0.81 (-0.01 and 0.29 g kg^{-1}) for specific humidity (numbers in parenthesis are the bias estimated from the difference of the daily mean values (ERA-Interim – ship data) and the root mean square error, respectively). In particular, variations in SLP for both datasets are almost coincident, showing that the ERA-Interim dataset could reproduce cyclone events in this region well. Since it is known that the precipitation in this region is primarily controlled by cyclone activities (Cullather et al., 1998), it is expected that the net precipitation can be estimated well from ERA-Interim data if the moisture flux given by $q\vec{V}$ is also accurately reproduced. Therefore we check the validity of q and the wind components next.

As for q, the average for ERA-Interim is 1.77 ± 0.31 g kg^{-1}, which is almost coincident with 1.78 ± 0.48 g kg^{-1} observed on the ship. Regarding wind, both directional components are slightly underestimated for the ERA-Interim compared with the ship-based data (Fig.4). This is probably because the anemometer of the *R/V Aurora*

291 *Australis* is installed at 30 m above sea level, while the surface wind level for ERA-
292 Interim is 10 m. According to boundary layer theory, the aerodynamic roughness length
293 is of the order of 0.1-1 cm for undeformed sea ice and 1-10 cm for deformed sea ice
294 (Leppäranta, 2005). If the mean horizontal wind speed is assumed to increase
295 logarithmically with height, as is typical for the neutral atmospheric condition, it
296 follows that the wind speed monitored at 30 m a.s.l. can be greater by 10-20% at most
297 than that at 10 m a.s.l., which can explain the difference between the two datasets. Thus,
298 we consider that ERA-Interim reproduced both components of the real surface wind
299 well in this region. This also justifies the lack of correction made to the ERA-Interim
300 wind speed.

301 Next, to validate the *P-E* obtained by this method, the annual mean for each grid cell
302 and for the period of 1990 to 2012 is plotted in Fig. 5. The spatial distribution of *P-E* in
303 Fig.5 is characterized by relatively high values off Wilkes Land, East Antarctica and
304 west of the Antarctic Peninsula (600-800 kg m^{-2} yr^{-1}) and relatively low values in the
305 Weddell and Ross seas (100-300 kg m^{-2} yr^{-1}). These values are similar to those from
306 past studies estimated by the moisture budget using meteorological dataset (Cullather et
307 al., 1998; Massom et al., 2001) and the glaciological dataset on Antarctica (Favier et al.,
308 2013; Giovinetto and Bentley, 1985; Lanaerts et al., 2012; Vaughan et al., 1999). Thus,
309 we assume that our method can reproduce the real net precipitation to some extent.

310 Finally, we check the *P-E* values calculated by this method against the ERA-Interim
311 snowfall product. A comparison of both datasets for 2007 and 2012 in the observation
312 area shows that while they had similar seasonal variations in both years, the annual
313 snowfall amount was larger than the calculated *P-E* by about 200 kg m^{-2} yr^{-1}. Whereas
314 the snowfall amount is 827 kg m^{-2} yr^{-1} (2007) and 846 kg m^{-2} yr^{-1} (2012), the calculated

315 *P-E* is 620 kg m^{-2} yr^{-1} (2007) and 625 kg m^{-2} yr^{-1} (2012). If we assume that the
316 difference between these datasets came from sublimation, the value of about 200 kg m^{-2}
317 yr^{-1} corresponds to about 18 W m^{-2} of the upward latent heat flux on the surface, which
318 is similar to the value of 28 W m^{-2} estimated for the Antarctic pack-ice zone (ice
319 concentration > 85%) by Weller (1980). In fact, the difference between the snowfall
320 amount and the calculated *P-E* (207 kg m^{-2} yr^{-1} for 2007 and 221 kg m^{-2} yr^{-1} for 2012) is
321 almost coincident with the ERA-Interim evaporation product (194 kg m^{-2} yr^{-1} for 2007
322 and 211 kg m^{-2} yr^{-1} for 2012). This supports our calculation method.
323
324 **4. Results**
325 **4.1 Meteorological conditions**
326 Time series of near-surface pressure (p_s), air temperature (T_a) and wind components
327 (U, V) monitored on the ship while in the sea-ice area are presented in Fig. 3. It is noted
328 that p_s, T_a and (U, V) varied with high amplitude, associated with the occasional passage
329 of cyclones. This situation is similar to past results in this region during 1995 (Massom
330 et al., 1998), 2003 (Massom, unpublished data), and 2007 (Toyota et al., 2011). T_a
331 ranged from -25 to 0^{o}C, and diurnal variability of up to several degrees began to appear
332 from early October; this compares to a variation of ~5 to 10 K associated with cyclonic
333 activity which has a period longer than several days. The zonal wind component (U),
334 ranging from -20 to 10 m s^{-1}, was generally stronger than the meridional wind
335 component (V) (-5 to 10 m s^{-1}), indicating the dominance of the circumpolar winds.
336 Wind speed in the 2012 observation period often exceeded 10 m s^{-1} but seldom
337 reached 20 m s^{-1}. The average was 6.9±4.3 m s^{-1}, which is somewhat weaker than the
338 9.7±5.8 m s^{-1} observed in the same region in 2007. Even when a strong wind (>10 m

339 s^{-1}) was blowing, it was less persistent in late winter to spring than in past years i.e.,
340 1995 (Massom et al., 1998) and 2007 (Toyota et al., 2011).

341 Regarding lateral snow redistribution across the sea ice, past observations have
342 shown that unconsolidated snow begins to drift at a wind speed of 5 m s^{-1}, and that
343 snow drifting almost always occurs when the wind speed at 5 m exceeds 8 m s^{-1}
344 (Andreas and Claffey, 1995). Moreover, drift-snow transport increases nearly
345 exponentially with wind speed (Budd et al., 1966; Takeuchi, 1980). Therefore, taking
346 into account the altitude of the anemometer on the ship, in our case wind speeds of 5 m
347 s^{-1} and 10 m s^{-1} are taken to be good indicators for the onset of snow drift and
348 significant drift-snow transport, respectively. Based on measurements every 10 minutes,
349 wind speeds of > 5 m s^{-1} were recorded for 59% of the observation period in 2012,
350 compared to ~83% in 1995 (Massom et al., 1998) and 72% in 2007. Moreover, wind
351 speeds of >10 m s^{-1} were less frequent in 2012 (21%) than in 2007 (44%). Therefore,
352 drift-snow transport in this region may be less of a factor in 2012, compared to previous
353 observations.

354

355 **4.2 Statistics of snow and sea ice**

356 Transect measurements during SIPEX II yielded mean ice thickness, freeboard, and
357 snow depths of 2.33±1.64 m (n = 447), 0.12±0.18 m (n = 442), and 0.45±0.26 m (n
358 = 1106), respectively. The relatively high sd values indicate that both ice and snow
359 thickness distributions were highly heterogeneous. Results obtained from the 11 transect
360 lines and 18 snow pits are listed in Table 1. For comparison, past statistical data
361 obtained in winter off East Antarctica are also shown in Table 2, revealing that while
362 such a high heterogeneity is similar to previous results i.e., in 1995 (Massom et al.,

1998), during ARISE 2003 (Massom, unpublished), and during SIPEX in 2007 (Toyota et al., 2011), the mean values of ice thickness, freeboard, and snow depth are all significantly larger in 2012. Moreover, Table 1 shows that this feature is common for almost all of the transect lines in 2012. In particular, the mean snow depth of 0.45 m is about three times deeper than that previously recorded in situ in the region. The relatively high mean snow thickness of 0.21±0.18 m in 2003 is composed of mean snow depths of 0.36±0.22 m (n = 2947) for rough ice and 0.17±0.16 m (n = 1909) for smooth ice (Massom et al., 2006). Impressively, the mean snow depth of 0.45 m in 2012 is even larger than that for the rough ice class in 2003.

To examine the snow conditions in more detail, the histograms of snow depth and sea ice thickness are analyzed for 2007 and 2012 (Fig.6 and Fig.7, respectively). Figure 6 shows a significant difference in snow-depth distribution between these two years. In 2007, there is a prominent peak at 0.05-0.10 m and the frequency decreases exponentially with increasing snow depth (to a maximum of 0.65-0.70 m). In 2012, on the other hand, the distribution is multi-modal and flatter, with a significant proportion of the snow being between 0.50-1.00 m. Similar properties are found for the sea-ice thickness distribution (Fig.7). Whereas a prominent peak appears at 0.6-0.8 m and the frequency decreases rapidly with ice thickness in 2007, the modal thickness is 1.0-1.2 m with a more gradual decrease with thickness in 2012. Taken together, these results suggest a relationship between the unusual ice-thickness distribution and the extraordinary snow depth in 2012.

To examine this, the correlation coefficients among ice thickness, snow depth, freeboard, and surface elevation are shown in Table 3, compared to 2007. One of the most prominent differences between these two years is that the correlation between

snow depth and ice thickness is non-significant in 2012 unlike 2007 i.e., r= 0.38 versus 0.82, respectively (Tab. 3). In general and on a scale of ~100 m, the mean snow depth on Antarctic sea ice tends to be highly correlated with the mean ice thickness (Jeffries et al., 1998; Toyota et al., 2011; Worby et al., 1996). This is because the freeboard of Antarctic sea ice is often near zero and the ratio of snow depth to ice thickness is kept almost constant due to the transformation of snow into snow ice when excessive snow loading induces negative freeboard (Jeffries et al., 1998; Maksym and Markus, 2008). Given the high mean freeboard (0.12 m) accompanied by significantly thicker ice (mean 2.33 m) in 2012, the lower correlation between snow depth and ice thickness suggests that the above process, associated snow-ice formation, was less of a factor in 2012. Significantly lower salinity in the basal snow layer (6.8) in 2012, compared with the values (13-17) in past observations (Tab. 2), also supports this hypothesis. This is because the salinity of the basal snow layer is largely determined by the infiltration of flooded seawater or capillary suction of brine from the ice surface (Sturm and Massom, 2010) and the wet saline layer is considered to lead to snow-ice formation.

Our results (Tab. 3) also suggest that the high freeboard in 2012 may have affected snow depth in another way. In general, higher freeboard often accompanies the increase in ice surface roughness (i.e., sd of freeboard) as deformation processes play a key role in the ice thickening process in the Antarctic seasonal ice zone (Worby et al., 1996), and ice thickness (and freeboard) is highly correlated with ice-surface roughness (Toyota et al., 2011). This is confirmed by the high correlation of *Hi* with the mean and sd of *Fb* (Tab. 3). Taken together, these results strongly suggest that enhanced ice-surface roughness in 2012, produced by enhanced deformation, strongly affected the snow redistribution to contribute to the significantly different snow-depth distribution (Fig. 6).

411 This is supported by the poor correlation between mean snow depth and sd of surface
412 elevation (r= 0.18) in 2012 compared with 2007 (r= 0.81) in Table 3 because the snow
413 redistribution is considered to be affected by the roughness of surface elevation. The
414 high degree of deformation in 2012 is also confirmed by the enhanced keel variation of
415 the underside of sea ice measured with an Autonomous Underwater Vehicle during the
416 same cruise (Williams et al., 2015).

417 In summary, two possible processes for the extraordinary snow conditions in 2012
418 are suggested from the statistics of snow and sea ice conditions: a reduction in snow ice
419 formation and a change in snow redistribution processes.

420

421 **4.3 Estimates of snow ice thickness and ice age**

422 Here we estimate the thickness of snow-ice layers from the samples collected to
423 quantify the snow-ice formation for each year. The analysis of 32 ice samples in 2007
424 showed that core length ranged from 0.19 m to 1.86 m with the average being 0.85±0.44
425 m. Since this is close to the mean ice thickness along the transects (i.e., 0.98±0.58 m;
426 Tab. 2), estimates of snow-ice can be regarded as being representative. Snow-ice layers
427 were present in 27 (84.4%) of the samples, mostly at the top of the ice cores, and their
428 thickness ranged from zero to 0.38 m with the average being 0.13±0.14 m. The fraction
429 of total snow-ice layers to ice-core length is 15.0% i.e., 4.10 m versus 27.28 m. This
430 value is comparable with past results obtained in this region (about 13%; Worby et al.,
431 1998).

432 By comparison and for the 7 ice samples in 2012, core lengths ranged from 0.82 m
433 to 1.95 m with the average being 1.20±0.39 m, somewhat thicker than in 2007.
434 Snow-ice layers were present in only 2 (28.6%) of the samples, and only at the top of

435 the ice cores. The thicknesses of snow-ice layers ranged from zero to 0.30 m, with the
436 average being 0.06±0.11 m, which is nearly half that in 2007. In 2012, the fraction of
437 total snow-ice layer (0.40 m) to total ice-core length (8.37 m) was 4.8%, which is also
438 significantly lower than that in 2007 (and past results). Thus, it is found that limited
439 snow-ice formation occurred in 2012 compared with past observations. This is
440 consistent with the results shown in the previous section.

441 When comparing spatially- and/or temporally-separated observations of sea ice and
442 overlying snow properties, we also need to consider the age of the ice floes on which
443 the samples were collected. For this purpose, bulk ice salinity of an ice core is a good
444 indicator because it decreases with the increase of ice age (approximated by thickness)
445 due to brine drainage and is significantly reduced due to the flushing process after
446 surviving the summer (Untersteiner, 1968). Thus the bulk ice salinity of second-year ice
447 is usually much lower (1-3 psu) than that of first-year ice (4-15 psu) (Cox and Weeks,
448 1974; Kovacs, 1996). Therefore we calculated bulk ice salinity for each sample; this is
449 plotted as a function of ice thickness (Fig.8), showing that bulk salinity ranges from 4 to
450 10 with a weak negative correlation with ice thickness (r = -0.32), and when averaged
451 for the ice samples thicker than 1 m, it is 5.12±1.11 for 2012, which is almost the same
452 as 5.53±1.11 for 2007. This result indicates that all of the ice samples collected in 2007
453 and 2012 can be regarded as first-year ice and there is no significant difference in ice
454 age between these two years.

455

456 **4.4 Net snow-accumulation rate**

457 Next, we estimate $\overline{\langle P \rangle} - \overline{\langle E \rangle}$ in Eq.2 using the ERA-Interim meteorological data.
458 The time series averaged over the observational area (Fig. 1) in 2007 and 2012 are

459 shown in Fig. 9. Sea-level pressure varied by up to 5-10 hPa with a period of several
460 days (Fig. 9a), especially in winter as a result of strong cyclonic activity in this region
461 (as shown by Jones and Simmonds [1993]). Associated with this, SAT (Fig. 9b) and *PW*
462 (Fig. 9c) also varied highly in autumn to winter in both years. The fact that the SAT was
463 negative throughout the winter, as shown in Fig.9b, justifies our assumption that the loss
464 of snow due to melting is negligible at this time. It is noteworthy that in winter, the SAT
465 varied from about -24^{o}C to nearly -1^{o}C, accompanied by high variability in *PW* ranging
466 from 1 kg m^{-2} to 12 kg m^{-2}. Therefore, although overall *PW* is lower in autumn to winter
467 than in summer, the calculated *P-E* tends to have a larger value in autumn compared to
468 winter with a noticeable peak in early winter (Fig. 9d) , as previously shown by
469 Cullather et al.(1998), Ligtenberg et al. (2012), and Yamazaki (1992). It is important to
470 note in Fig. 9 that there are no significant differences either in the meteorological
471 conditions or *P-E* between 2007 and 2012.

472 Monthly values of *P-E* in 2007 and 2012, plotted with the 1990-2012 average in
473 Fig.10a, show both a characteristic seasonal variation of *P-E* in this observational
474 region and no significant difference of *P-E* in winter between 2012 and 2007 as far as
475 the observational region is concerned. The total *P-E* from May to September was
476 estimated to be 313±49 kg m^{-2} on average (1990-2012), and the values of 292 kg m^{-2} in
477 2007 and 325 kg m^{-2} in 2012 are both within a sd of the average. Although the value in
478 2012 is somewhat larger than that in 2007, the difference of 33 kg m^{-2} in water
479 equivalent corresponds to only 0.03 m in snow depth, when weighted by the snow
480 density for the individual year. This is insufficient to explain the observed difference in
481 snow depth (i.e., 0.31 m) between 2007 and 2012. To examine this for other years, the
482 interannual variability of *P-E* during winter is plotted in Fig.10b. It is shown here that

483 the *P-E* in 1992, 1994, and 1995 (when observations were conducted off East
484 Antarctica) was larger than that in 2012. Thus, these results indicate that *P-E* is not a
485 controlling factor which contributed to the difference in the snow-accumulation rate on
486 sea ice.

487 Next, to examine the difference between 2007 and 2012 on a larger scale, we plotted
488 the circum Antarctic spatial pattern of winter *P-E* south of 60^{o}S (Fig.11). The general
489 feature is that *P-E* is relatively high in the regions west of the Antarctic Peninsula and
490 off East Antarctica, and relatively low in the Ross and Weddell seas in both years. This
491 spatial pattern is consistent with past results using the meteorological datasets (Cullather
492 et al., 1998; Massom et al., 2001). At the same time, Figure 11 shows no significant
493 difference in *P-E* within the observation area between these two years - although in the
494 region between 150^{o} and 180^{o}E (east of the observation area), there is a higher *P-E* area
495 in 2012. However, in light of the fact that the monthly mean zonal component of wind
496 in the observation area was about -2 m s-1 in 2012, the eastward ice drift is estimated to
497 be approximately 777 km (14 degrees) at most, assuming that the Nansen number (the
498 ratio of ice drift to wind speed) is 3% (Leppäranta, 2005). Therefore it is unlikely that
499 our measurements were affected by this high *P-E* area.

500 To place the above results in longer-term context, mean *PW* and mean *P-E* in each
501 winter over 1990-2012 and for the five Antarctic sectors (from Fig. 1) are plotted in Fig.
502 12. Although mean *PW* is highest in the Bellingshausen and Amundsen seas sector, *P-E*
503 is consistently by far the largest in the SW Pacific Ocean sector (including off Wilkes
504 Land), again reflecting the strong cyclonic activity there (Jones and Simmonds, 1993).
505 Mean *P-E* values in winter for the total period are i) Indian Ocean: 202±24 kg m^{-2}; ii)
506 SW Pacific Ocean: 286 ± 26 kg m^{-2}; iii) Ross Sea: 211 ± 14 kg m^{-2}; iv)

507 Amundsen-Bellingshausen seas: 174±25 kg m^{-2}; and v) Weddell Sea: 144±15 kg m^{-2}.
508 The values of mean *P-E* in winter for the individual sectors in 2012 (i.e., 194, 308, 220,
509 176, and 144 kg m^{-2} for the same sectors, respectively) are all within one sd of the
510 average, and there is no evidence that the precipitation in 2012 was significantly higher
511 or lower in any sector around Antarctica.
512
513 **4.5 Snow-mass balance**
514 In this section, we synthesize the results to throw light on the most likely causes of
515 the unusually large mean snow depths observed in 2012 from the snow mass balance
516 equation of Eq.2. Direct comparison with 2007, when similar data were available, sheds
517 light on this. In fact, the mean snow depth, *P-E*, and snow ice thickness estimated for
518 2007 were similar to past observations – again highlighting the unusual nature of snow
519 conditions in 2012 in the SIPEX II experimental region off Wilkes Land (East
520 Antarctica). The results obtained for both years are listed in Table 4, where $\overline{\langle B \rangle}$ was
521 given by the mean snow depths observed, and $\overline{\langle P \rangle} - \overline{\langle E \rangle}$ was calculated by integrating
522 the daily *P-E* (s.w.e.) in the observation area for the winter (May to September) and
523 dividing it by the mean snow density of each year. Although the area for integration was
524 fixed to a relatively limited region, values of $\overline{\langle P \rangle} - \overline{\langle E \rangle}$ obtained (i.e., 292 kg m^{-2} for
525 2007 and 325 kg m^{-2} for 2012) are close to those for a wider SW Pacific sector (of 289
526 kg m^{-2} for 2007 and 308 kg m^{-2} for 2012). $\overline{\langle I \rangle}$ was estimated from Eq.6, where h_{si} is
527 given by the mean thickness of the estimated snow-ice layers.
528 In Table 4, it is noticeable that in both years the value of $\overline{\langle L \rangle}$ represents nearly half
529 or more fraction of $\overline{\langle P \rangle} - \overline{\langle E \rangle}$. This suggests that a significant amount of the net
530 precipitation is lost to leads and cracks due to snow drift. This is consistent with past

studies. Eicken et al. (1994) estimated a loss of snow into leads of 100 kg m^{-2} yr^{-1} (nearly half of the annual *P*-*E*) in the Weddell Sea, and Leonard and Maksym (2011) modeled snow loss into leads of >50% over the entire Antarctic sea ice zone. It is important to note in Table 4 that although each term of $\overline{\langle P \rangle} - \overline{\langle E \rangle}$, $\overline{\langle I \rangle}$, and $\overline{\langle L \rangle}$ contributed partially (0.03 m, 0.10 m, and 0.18 m, respectively) to the enhancement in $\overline{\langle B \rangle}$ (0.31 m) in 2012, $\overline{\langle L \rangle}$ is the most important factor among them. This indicates that while the restriction of snow ice formation due to higher freeboard affected the mean snow depth, the snow redistribution due to snow drift and the resultant loss of snow into leads was more important in driving the snow depth distribution on the sea ice in this region and at this time.

However, it should be kept in mind that the relative importance of $\overline{\langle P \rangle} - \overline{\langle E \rangle}$, $\overline{\langle I \rangle}$, and $\overline{\langle L \rangle}$ may change somewhat according to physical parameters although the significant contribution of $\overline{\langle L \rangle}$ is true. For example, if a snow density of 336 kg m^{-3} (the average of 2007 and 2012), was used for both years, the *P*-*E* contribution in the snow volumetric balance difference between these two years would have a value of 0.10 m, leading to evenly distributed contributions of $\overline{\langle P \rangle} - \overline{\langle E \rangle}$ (= 0.10 m), $\overline{\langle I \rangle}$ (= 0.10 m), and $\overline{\langle L \rangle}$ (= 0.11 m) to the observed difference of $\overline{\langle B \rangle}$ (= 0.31 m).

4.6 Possible processes for controlling $\overline{\langle L \rangle}$

Next, we examine what caused the difference in $\overline{\langle L \rangle}$ in 2012. The significant difference in the histogram of snow depth in Fig. 6 also suggests a difference in the snow redistribution process due to snow drift between these two years. There seem to be two possibilities: one is the meteorological conditions, especially wind speed, and the other is the surface conditions of the sea ice, related to the ice thickening process as

555 discussed in Section 4.2. Regarding wind speed, it was pointed out in Section 4.1 that
556 the ship-based mean wind speed was somewhat weaker in 2012 than in 2007. As snow
557 transport due to drift increases with increasing wind speed (Budd et al., 1966; Takeuchi,
558 1980), weaker prevailing wind conditions over a wider region and for an extended
559 season could possibly have affected $\overline{\langle L \rangle}$. However, there is no evidence in the time
560 series of the monthly mean wind speed averaged over the observation area that the wind
561 speed in 2012 was significantly weaker compared with other years (Fig. 13a). There
562 may be a possibility that ERA-Interim could not accurately reproduce the real wind
563 speed. Even so, in light of the fact that even in the years when the mean wind speed was
564 stronger than in 2007 (i.e. 1994, 1995, 2003) the mean snow depth was kept almost
565 constant, it is unlikely that the wind speed was a controlling factor. Therefore, it is more
566 likely that the significantly lower $\overline{\langle L \rangle}$ in 2012 is attributable to sea ice surface
567 conditions.

568 Two types of such conditions could affect $\overline{\langle L \rangle}$: the surface roughness and the
569 spacing and width of the leads, both of which are closely related to sea ice deformation.
570 The first condition was already discussed in Section 4.2. Regarding the latter one, the
571 spacing distribution of leads is considered to be closely related to floe size distribution.
572 To qualitatively compare the floe size distributions between 2007 and 2012, NASA
573 MODIS satellite images extracted from exactly the same region (Fig. 1) are shown in
574 Fig. 14. Note that the regions of the two images are exactly the same but separated by
575 about a month (due to cloud cover limitations). Considering that sea-ice extent is almost
576 stable in September to October, however, it should be considered that these images
577 represent the ice conditions in the winter of each year to some extent. Although it is
578 difficult to estimate the floe-size distribution exactly using this imagery, a comparison

of the two images shows that overall the floe size in the observation area was larger in 2012 than in 2007. This may be explained as follows: according to Fig.14, sea-ice extent was greater in 2012 than in 2007 and consequently the observation area was further poleward from the ice edge in 2012, and thus less affected by breakup due to waves penetrating from the open ocean. It is likely that such large ice floes in 2012 reduced the opportunity for blowing snow particles to enter leads, resulting in the significant reduction of $\langle L \rangle$. To confirm this, we compare the sea-ice edge contours for all the years with East Antarctic observations (Fig.15). It is shown that extensive sea ice coverage off East Antarctica especially in 2003 and 2012, coincided with relatively deep snow observation (Table 2). In light of the fact that the mean ice thickness was much thicker and the ice surface was much rougher in 2012 compared to 2003, this may support our speculation that the effects of rough ice surface and large floe-size distribution are both important to the abnormally deep snow in 2012.

Based on all these results, we deduce that rougher ice surface caused by highly active deformation processes and larger floe conditions associated with a wider expansion of the sea-ice area are mostly responsible for the extraordinarily deep snow in 2012.

5. Summary and discussion

During the SIPEX II voyage off Wilkes Land, East Antarctica in late winter 2012, we encountered unprecedented deep snow on sea ice. The mean snow depth measured along transects on five ice floes amounted to 0.45 ± 0.26 m, nearly three times the values of past observations in this region. In this paper we examined what caused such extraordinary snow conditions, based on the snow-mass balance which is composed of

603 snow accumulation on sea ice $\overline{\langle B \rangle}$, net precipitation $\overline{\langle P \rangle}$-$\overline{\langle E \rangle}$, consumption into snow
604 ice formation $\overline{\langle I \rangle}$, and loss into leads due to snow drift $\overline{\langle L \rangle}$ during the winter (May to
605 September). In the estimation of each term, net precipitation was calculated from the
606 moisture budget equation, using the ERA-Interim Reanalysis dataset. Although it is
607 difficult to estimate the exact accuracy of the calculated $\overline{\langle P \rangle}$-$\overline{\langle E \rangle}$, the ERA-Interim
608 reproduced the real surface air temperature, pressure, humidity, and wind well.
609 Moreover, the spatial distribution of the annual $\overline{\langle P \rangle}$-$\overline{\langle E \rangle}$ averaged for the period of
610 1990 to 2012 matched well with past results (Cullather et al., 1998) and was consistent
611 with the estimates from glaciological data for the Antarctic (Giovinetto and Bentley,
612 1985). $\overline{\langle I \rangle}$ was estimated based on the ice core samples collected in 2007 and 2012,
613 while $\overline{\langle L \rangle}$ was estimated as the residual of the snow-mass balance. Since $\overline{\langle I \rangle}$ was
614 obtained in 2007 and 2012, our discussion was focused mainly on the comparison
615 between these two years, with 2007 assumed to be typical of past observations.
616 From the analysis of $\overline{\langle P \rangle}$-$\overline{\langle E \rangle}$ using the ERA-Interim dataset for 1990 to 2012, there
617 appears to be no evidence for a significantly greater amount of net precipitation in 2012
618 compared with other years, not only for the limited observation area but also for the
619 wider area off East Antarctica. These results indicate that on both local and hemispheric
620 scales the precipitation amount in winter 2012 was not significantly different from past
621 years and therefore it is unlikely that *P-E* was a controlling factor which caused the
622 anomalously deep snow in 2012. On the other hand, the SIPEX II observations were
623 characterized by significantly thick sea ice. The mean ice thickness measured along the
624 transects amounted to 2.33±1.64 m, more than twice the thickness obtained by past
625 observations. Significantly thick ice accompanied much higher freeboard (0.12±0.18
626 m), which acted to reduce the snow ice formation. Indeed, it was revealed from the

627 analysis of ice-core samples that the mean thickness of snow-ice layers was 0.06±0.11
628 m in 2012, nearly half the value of 0.13±0.14 m in 2007. This means that $\overline{\langle I \rangle}$ was
629 reduced in 2012 as compared to 2007. Although this effect contributed partly to the
630 increase in mean snow depth in 2012, it is still not enough to explain the difference of
631 mean snow depth between these two years. By substituting these results into Eq.2, it
632 was found that $\overline{\langle L \rangle}$ amounts to 0.57 m in 2007 and 0.39 m in 2012, nearly half or more
633 of $\overline{\langle P \rangle}$-$\overline{\langle E \rangle}$. This indicates that $\overline{\langle L \rangle}$ is a controlling factor of snow accumulation in both
634 years, and possibly worked most efficiently to produce the difference in mean snow
635 depth between 2007 and 2012.

636 As possible reasons for the significant difference in $\langle L \rangle$ between these two years,
637 there seem to be two factors which can affect $\overline{\langle L \rangle}$: the surface roughness and the
638 spacing and width of the leads, both of which are closely related to the sea ice growth
639 processes. Regarding rough surface conditions, the significantly thicker ice in 2012,
640 possibly produced by unusually rigorous deformation activities, accompanied very
641 rough ice surface. This is also confirmed by the much larger sd of freeboard in 2012
642 (0.18 m) compared with 2003 and 2007 (~0.10 m) in Table 2. It is possible that
643 enhanced surface roughness affected the snow redistribution and accumulation.

644 However, the reason for the highly active deformation processes of sea ice in 2012
645 remains unresolved. It is difficult to explain this simply from the interannual variability
646 in ERA-Interim wind speed or wind divergence on a grid scale (~100 km), which are
647 presumed to largely affect the deformation intensity, in light of the fact that they did not
648 show any significant and unusual features in 2012 (Fig.13).

649 On the other hand, the spacing and width of leads might have reduced the loss of
650 drifting snow into leads, with floe-size distribution affecting the observed snow depth

651 on the sea ice. Taken together, these results confirm earlier findings (e.g., Eicken et al.,
652 1994; Massom et al., 2006; Toyota et al., 2011; Leonard and Maksym, 2011) that
653 snow-sea ice interaction processes beyond snow-ice formation play a significant role in
654 determining the mean snow depth on Antarctic sea ice.

655 In this paper, we have focused on the fate of snow accumulated on sea ice on a scale
656 of more than 100 km. In addition, we would like to point out a localized feature of the
657 snow accumulation on sea ice from our observational results based on the fact that snow
658 accumulation often occurs on scales that are significantly smaller than the grid interval
659 of the ERA-Interim dataset. As an example, we show one result of the diurnal snow-pit
660 observations conducted on October 6-8 in 2012. Associated with a passage of a deep
661 low pressure system, strong southeasterly winds blew over this area (Fig. 3) and
662 significant precipitation occurred on October 7 (Fig. 9d). According to the diurnal
663 snow-pit measurements, snow depth increased from 0.41 m at 18:50 (LST) on October
664 6 to 0.65 m at 13:30 on October 8. The increase of 0.24 m in snow depth depressed the
665 snow/ice boundary by about 0.08 m and induced flooding of brine within sea ice on the
666 ice surface, accompanying an increase in basal snow layer salinity from 5.8 psu on
667 October 6 to 57.8 at 13:30 and even 69.1 at 18:45 on October 8. On this day, the
668 calculated mean P-E in the observational area is to be 7.4 kg m^{-2}, corresponding to only
669 0.02 m (Fig. 9d). This demonstrates a strong localized feature in the spatial distribution
670 of snow accumulation and the effect that it had on snow properties, reminding us that
671 the variability of snow properties on a small scale should be taken into account when
672 discussing the fate of snow on a regional scale.

673 Finally, although this study underlines the importance of snow-sea ice interactions
674 for determining the snow-depth distribution off East Antarctica, several questions

675 remain unanswered regarding what caused the strong sea-ice deformation off Wilkes
676 Land in the winter-spring of 2012, how much the surface roughness of sea-ice affects
677 drift-snow transport, and what caused such expansion of sea ice extent in 2012. To
678 address these questions will require further continuous observations and theoretical
679 studies on the relationship between snow accumulation/loss and sea ice surface
680 roughness, rheology and floe-size distribution on various scales, and in various seasons.
681

682 **Acknowledgments**

683 The authors deeply appreciate the support given by the captain, crew and scientists
684 aboard the R/V *Aurora Australis* during SIPEX II. Special thanks are given to the chief
685 scientist of SIPEX II, Dr. K. Meiners, for his dedicated assistance. We gratefully thank
686 C. Dietz and C. Cook (Central Science Laboratory, UTAS) for $\delta^{18}O$ measurements and
687 Dr. A. Moy (AAD) for further processing and collating the $\delta^{18}O$ data. Discussions with
688 Dr. T. Maksym and Dr. G. Williams were very helpful. Comments by two anonymous
689 reviewers were also helpful to improve the paper. This work was supported by AAS
690 4073 and partly by JSPS KAKENHI 21510002 [Grant-in-Aid for Scientific Research
691 (C)] for TT and 25·03748 for AF, and by the Australian Government's Cooperative
692 Research Centre program through the Antarctic Climate & Ecosystems Cooperative
693 Research Centre. For RM and PH, the work contributes to AAS projects 4116 and 4072
694 and 4301, respectively.
695

Reference

Andreas, E.L., K.J. Claffey, 1995. Air-ice drag coefficients in the western Weddell Sea. 1. Values deduced from profiles measurements. *Journal of Geophysical Research*, 100(C3), 4821-4831.

Bromwich, D.H., 1988. Snowfall in high southern latitudes. *Reviews of Geophysics*, 26(1), 149-168.

Bromwich, D.H., 1990. Estimates of Antarctic precipitation. *Nature*, 343, 627-629.

Bromwich, D.H., F.M. Robasky, R.I. Cullather, M.L. Van Woert, 1995. The atmospheric hydrologic cycle over the Southern Ocean and Antartica from operational numerical analyses. *Monthly Weather Review*, 123, 3518-3538.

Budd, W.F., W.R.J. Dingle, U. Radok, 1966. The Byrd snow drift project: Outline and basic results. In "Studies in Antarctic Meteorology", *Antarctic Research Series*, 9, edited by M.J. Rubin, American Geophysical Union, Washington, D.C., 71-134.

Cox, G.F.N., W.F. Weeks, 1974. Salinity variations in sea ice. *Journal of Glaciology*, 13, 109-120.

Cullather, R.I., D.H. Bromwich, M.L. Van Woert, 1998. Spatial and temporal variability of Antarctic precipitation from atmospheric methods. *Journal of Climate*, 11, 334-367.

Eicken, H., 1992. The role of sea ice in structuring Antarctic ecosystems. *Polar Biology*, 12, 3-13.

Eicken, H., M.A. Lange, H.-W. Hubberten, P. Wadhams, 1994. Characteristics and distribution patterns of snow and meteoric ice in the Weddell Sea and their contribution to the mass balance of sea ice. *Ann. Geophysicae*, 12, 80-93.

720 Favier, V., C. Agosta, S. Parouty, G. Durand, G. Delaygue, H. Gallee, A.-S. Drouet,
721 A. Trouvilliez, G. Krinner, 2013. An updated and quality controlled surface mass
722 balance dataset for Antarctica. *The Cryosphere*, 7(2), 583-597.
723 Fichefet, T., M.A. Morales Maqueda, 1999. Modelling the influence of snow
724 accumulation and snow-ice formation on the seasonal cycle of the Antarctic sea-ice
725 cover. *Climate Dynamics*, 15, 251-268.
726 Fierz, C., R.L. Armstrong, Y. Durand, P. Etchevers, E. Greene, D.M. McClung, K.
727 Nishimura, P.K. Satyawali, S.A. Sokratov, 2009. *The International Classification for*
728 *Seasonal Snow on the Ground*. IHP-VII Technical Documents in Hydrology No83,
729 IACS Contribution No1, UNESCO-IHP, Paris, 80pp.
730 Giovinetto, M.B., C.R. Bentley, 1985. Surface balance in ice drainage systems of
731 Antarctia. *Antarct. J. U.S.*, 20, 6-13.
732 Ishii, H., T. Toyota, 2012. Temporal evolution of the structural properties of seasonal sea
733 ice during the early melt season. *Journal of Glaciology*, 58(207), 23-37.
734 Jeffries, M.O., R.A. Shaw, K. Morris, A.L. Veazey, H.R. Krouse, 1994. Crystal
735 structure, stable isotopes (d18O), and development of sea ice in the Ross,
736 Amundsen, and Bellingshausen seas, Antarctica.
737 *Journal of Geophysical Research*, 99 (C1), 985-995.
738 Jeffries, M. O., A. P. Worby, K. Morris, W. F. Weeks, 1997. Seasonal variations in the
739 properties and structural an isotopic composition of sea ice and snow cover in the
740 Bellingshausen and Amundsen Seas, Antarctica.
741 *Journal of Glaciology*, *43*, 138-151.
742 Jeffries, M.O., S. Li, R.A. Jana, H.R. Krouse, B. Hurst-Cushing, 1998. Late winter
743 first-year ice profile thickness variability, seawater flooding and snow ice formation

744 in the Amundsen and Ross Seas. *Antarctic Research Series*, 74, 69-87, AGU.
745 Jeffries, M.O., H.R. Krouse, B. Hurst-Cushing, T. Maksym, 2001. Snow-ice accretion
746 and snow-cover depletion on Antarctic first-year sea-ice floes. *Annals of Glaciology*,
747 33, 51-60.
748 Jones, D.A., I. Simmonds, 1993. A climatology of Southern Hemisphere extratropical
749 cyclones. *Climate Dynamics*, 9, 131-145.
750 Kanna, N., T. Toyota, J. Nishioka, 2014. Iron and macro-nutrient concentrations in sea
751 ice and their impact on the nutritional status of surface waters in the southern
752 Okhotsk Sea. *Progress in Oceanography*, 126, 44-57.
753 Kovacs, A., 1996. Sea Ice. Part I. Bulk salinity versus ice floe thickness. USA Cold
754 Regions Research and Engineering Laboratory, *CRREL Report*, 97-7, 1-16.
755 Lecomte, O., T. Toyota, Influence of wet conditions on snow temperature diurnal
756 variations: An East-Antarctic sea ice case study. *Deep-Sea Research II* (this issue).
757 Ledley, T.S., 1991. Snow on sea ice: Competing effects in shaping climate.
758 *Journal of Geophysical Research*, 96(D9), 17,195-17,208.
759 Lenaerts, J.T.M., M.R. vanden Broeke, W.J. van deBerg, E. van Meijaard, P.K.
760 Munneke, 2012. A new, high-resolution surface mass balance map of Antarctica
761 (1979-2010) based on regional atmospheric climate modeling.
762 *Geophysical Research Letters*, 39, L04501, doi:10.1029/2011GL050713.
763 Leonard, K.C., T. Maksym, 2011. The importance of wind-blown snow redistribution to
764 snow accumulation on Bellingshausen sea ice.
765 *Annals of Glaciology*, 52(57), 271-278.
766 Leppäranta, M., 2005. The drift of sea ice. Praxis Publishing Ltd, UK, pp.266.
767 Leppäranta, M., P. Kosloff, 2000. The structure and thickness of Lake Pääjärvi ice.

Geophysica, 36, 233-248.

Ligtenberg, S.R.M., M. Horwath, M.R. van den Broeke, B. Legresy, 2012: Quantifying the seasonal “breathing” of the Antarctic ice sheet. *Geophysical Research Letters*, 39, L23501, doi:10.1029/2012GL053628.

Maksym, T., M.O. Jeffries, 2000. A one-dimensional percolation model of flooding and snow-ice formation on Antarctic sea ice. *Journal of Geophysical Research*, 105(C11), 26,313-26,331.

Maksym, T., T. Markus, 2008. Antarctic sea ice thickness and snow-to-ice conversion from atmospheric reanalysis and passive microwave snow depth. *Journal of Geophysical Research*, 113, C02S12, doi: 10.1029/2006JC004085.

Markus, T., D.J. Cavalieri, 1998. Snow depth distribution over sea ice in the Southern Ocean from satellite passive microwave data. In “Antarctic Sea Ice: Physical Processes, Interactions and Variability”, *Antarctic Research Series, 74*, edited by M.O. Jeffries. American Geophysical Union, Washington, D.C., 19-39.

Markus, T., R. Massom, A. Worby, V. Lytle, K. Nathan, T. Maksym, 2011. Freeboard, snow depth and sea-ice roughness in East Antarctica from in situ and multiple satellite data. *Annals of Glaciology*, 52(57), 242-248.

Massom, R.A., V.I. Lytle, A.P. Worby, I. Allison, 1998. Winter snow cover variability on East Antarctic sea ice. *Journal of Geophysical Research*, 103(C11), 24,837-24,855.

Massom, R.A., H. Eicken, C. Haas, et al., 2001. Snow on Antarctic sea ice. *Reviews of Geophysics*, 39, 413-445.

Massom, R. A., A.P. Worby, V.I. Lytle, T. Markus, I. Allison, T. Scambos, H. Enomoto, K. Tateyama, T. Haran, J.C. Comiso, A. Pfaffling, T. Tamura, A. Muto, P. Kanagaratnam, B. Giles, 2006. ARISE (Antarctic Remote Ice Sensing

792 Experiment) in the East 2003: Validation of satellite derived sea ice data products.
793 *Annals of Glaciology*, 44, 288-296.
794 Massom, R.A., P. Reid, S. Stammerjohn, B. Raymond, A. Fraser, S. Ushio, 2013.
795 Change and variability in East Antarctic sea ice seasonality, 1979/80-2009/10.
796 *PloS One*, 8 (5), e64756, doi:10.1371/journal.pone.0064756.
797 Nomura, D., J. Nishioka, M.A. Granskog, A. Krell, S. Matoba, T. Toyota, H. Hattori,
798 K. Shirasawa, 2010. Nutrient distributions associated with snow and sediment-laden
799 layers in sea ice of the southern Sea of Okhotsk. *Marine Chemistry*, 119, 1-8.
800 Powell, D.C., T. Markus, A. Stossel, 2005. Effects of snow depth forcing on Southern
801 Ocean sea ice simulation.
802 *Journal of Geophysical Research*, 110, C06001, doi:10.1029/ 2003JC002212.
803 Serreze, M.C., A.P. Barrett, A.G. Slater, M. Steele, J. Zhang, K.E. Trenberth, 2007.
804 The large-scale energy budget of the Arctic. *Journal of Geophysical Research*, 112,
805 D11122, doi: 10.1029/2006JD008230.
806 Sturm, M., R.A. Massom, 2010. Snow and Sea Ice. In D. Thomas and G. Dieckmann (editors),
807 *Sea Ice*, 2nd Edition, Wiley-Blackwell, Oxford, pp. 153-204.
808 Takeuchi, M., 1980. Vertical profile and horizontal increase of drift-snow transport.
809 *Journal of Glaciology*, 26(94), 481-492.
810 Toyota, T., T. Kawamura, Kay I. Ohshima, H. Shimoda, M. Wakatsuchi, 2004. Thickness
811 distribution, texture and stratigraphy, and a simple probabilistic model for dynamical
812 thickening of sea ice in the Sea of Okhotsk.
813 *Journal of Geophysical Research*, 109, C06001, doi:10.1029/2003JC002090.
814 Toyota, T., R. Massom, K. Tateyama, T. Tamura, A. Fraser, 2011. Properties of snow

overlying the sea ice off East Antarctica in late winter 2007. *Deep-Sea Research II*, 58, 1137-1148.

Toyota, T., I.J. Smith, A.J. Gough, P.J. Langhorne, G.H. Leonard, R.J. Van Hale, A.R. Mahoney, and T.G. Haskell (2013): Oxygen isotope fractionation during the freezing of seawater. *Journal of Glaciology*, 59(216), 697-710.

Trenberth, K.E., 1991. Climate diagnostics from global analyses: Conservation of mass in ECMWF analyses. *Journal of Climate*, 4, 707-722.

Untersteiner, N., 1968. Natural desalination and equilibrium salinity profile of perennial sea ice. *Journal of Geophysical Research*, 73(4), 1251-1257.

Vaughan, D.G., Bamber, J.L., Giovinetto, M., Russell, J., Cooper, A.P.R., 1999. Reassessment of net surface mass balance in Antarctica. *Journal of Climate*, 12, 933-946.

Weller, G., 1980. Spatial and temporal variations in the south polar surface energy balance. Monthly Weather Review, 108, 2006-2014.

Williams, G.D., T. Maksym, J. Wilkinson, C. Kunz, C. Murphy, P. Kimball, H. Singh, 2015. Thick and deformed Antarctic sea ice mapped with autonomous underwater vehicles. *Nature Geoscience*, 8, 61-67.

Worby, A.P., M.O. Jeffries, W.F. Weeks, K. Morris, R. Jana, 1996. The thickness distribution of sea ice and snow cover during late winter in the Bellingshausen and Amundsen Seas, Antarctica, *Journal of Geophysical Research*, 101, 28,441-28,455.

Worby, A.P., R.A. Massom, I. Allison, V.I. Lytle, P. Heil, 1998. East Antarctic sea ice: A review of its structure, properties and drift. In “Antarctic Sea Ice: Physical processes, interactions and variability”, *Antarctic Research Series, 74,* edited by M.O. Jeffries. American Geophysical Union, Washington, D.C., 41-67.

839 Worby, A.P., T. Markus, A.D. Steer, V.I. Lytle, R.A. Massom, 2008. Evaluation of
840 AMSR-E snow depth product over East Antarctic sea ice using in situ measurements
841 and aerial photography. *Journal of Geophysical Research*, 113, C05S94,
842 doi:10.1029/2007JC004181.
843 Yamazaki, K., 1992. Moisture budget in the Antarctic atmosphere,
844 *Proceedings of the National Institute of Polar Research (NIPR) Symposium on*
845 *Polar Meteorology and Glaciology*, 6, 36-45.
846
847

Figure captions:

Figure 1. Geographical map showing the location of the observation area.
The whole Antarctic area with the ERA-Interim grid cells used for analysis, and the five sectors used in the analysis. The thick solid line denotes the ice edge on September 30, 2012 (maximum).
(a) The square area off East Antarctica denotes the observational area in Fig. 1b.
(b) Magnified map around the observation area. The two square areas delineated by broken and solid lines depicts the observational area in Fig.1a and the MODIS images in Fig.14, respectively. The numbers denote the ice station number, while the asterisk shows the position of the ship when it was beset in the sea ice from October 26 to November 5, 2012.

Figure 2. The seasonal evolution of sea-ice extent around Antarctica in
(a) 2007 and (b) 2012.
The green, red, yellow, and blue lines denote the ice edge location on March 1, May 1, July 1, and September 1, respectively (based on 15% ice concentration). Note that the sea ice began to cover the observation area approximately after May in both years. The data source is
http://www.iup.uni-bremen.de/seaice/amsredata/asi_daygrid_swath/l1a/s6250/ for 2007 and http://www.iup.uni-bremen.de:8084/ssmisdata/asi_daygrid_swath/s6250 for 2012.

Figure 3. Comparison of ERA-Interim data and ship-based observations for
(a) sea level pressure; (b) surface air temperature;
(c) zonal component and (d) meridional component of surface wind;
(e) surface wind speed; (f) surface vapour pressure; and

872 (g) specific humidity at the surface.

873 Figure 4. Scatter plots comparing the ERA-Interim data and ship-based observations for

874 (a) daily mean zonal wind and (b) daily mean meridional wind.

875 Figure 5. Spatial distribution of annual net precipitation (*P-E*) averaged for the

876 period 1990 to 2012 around Antarctica south of 60^{o}S (in kg m^{-2} year^{-1}).

877 Figure 6. Histograms of snow depth measured *in-situ* along observational transect lines

878 in (a) 2007 and (b) 2012.

879 Figure 7. Histograms of sea-ice thickness measured *in-situ* along observational transect

880 lines in (a) 2007 and (b) 2012.

881 Figure 8. Scatter plots comparing bulk ice salinity and ice thickness.

882 In the figure, open circles denote 2007 samples and triangles 2012 samples.

883 Figure 9. Time series of (a) sea level pressure; (b) surface air temperature;

884 (c) precipitable water; and (d) *P-E*.

885 Thin and thick lines correspond to 2007 and 2012, respectively.

886 Figure 10. Time series of calculated *P-E* in the observational area.

887 (a) Seasonal variation of monthly *P-E* for 2012 (thick solid line), 2007

888 (thin solid line), and the average for the period 1990 to 2012 (broken line).

889 (b) Interannual variability of winter *P-E* (May to September) for the period

890 1990 to 2012. Open circles correspond to the years when the

891 snow observations were conducted (Table 2).

892 Figure 11. Spatial distribution of calculated *P-E* for the winters of (a) 2007 and (b) 2012

893 The square area denotes the observational area in 2007 and 2012.

894

895

Figure 12. Interannual variability of (a) *P-E* and (b) precipitable water for the individual Sectors marked on Fig. 1a. In Fig12a, “A&B” denotes Amundsen and Bellingshausen Seas.

Figure 13. Interannual variability in the ERA-Interim data for the period 1990 to 2012 for: (a) surface wind speed; and (b) divergence of the wind.

Figure 14. Satellite MODIS images showing the ice conditions on (a) September 10, 2007 and (b) October 5, 2012. See Fig.1b for the location of the images. The width of the images is approximately 750 km.

Figure 15. Satellite-derived sea-ice extent on September 30 in the years when observational programmes were conducted off East Antarctica.

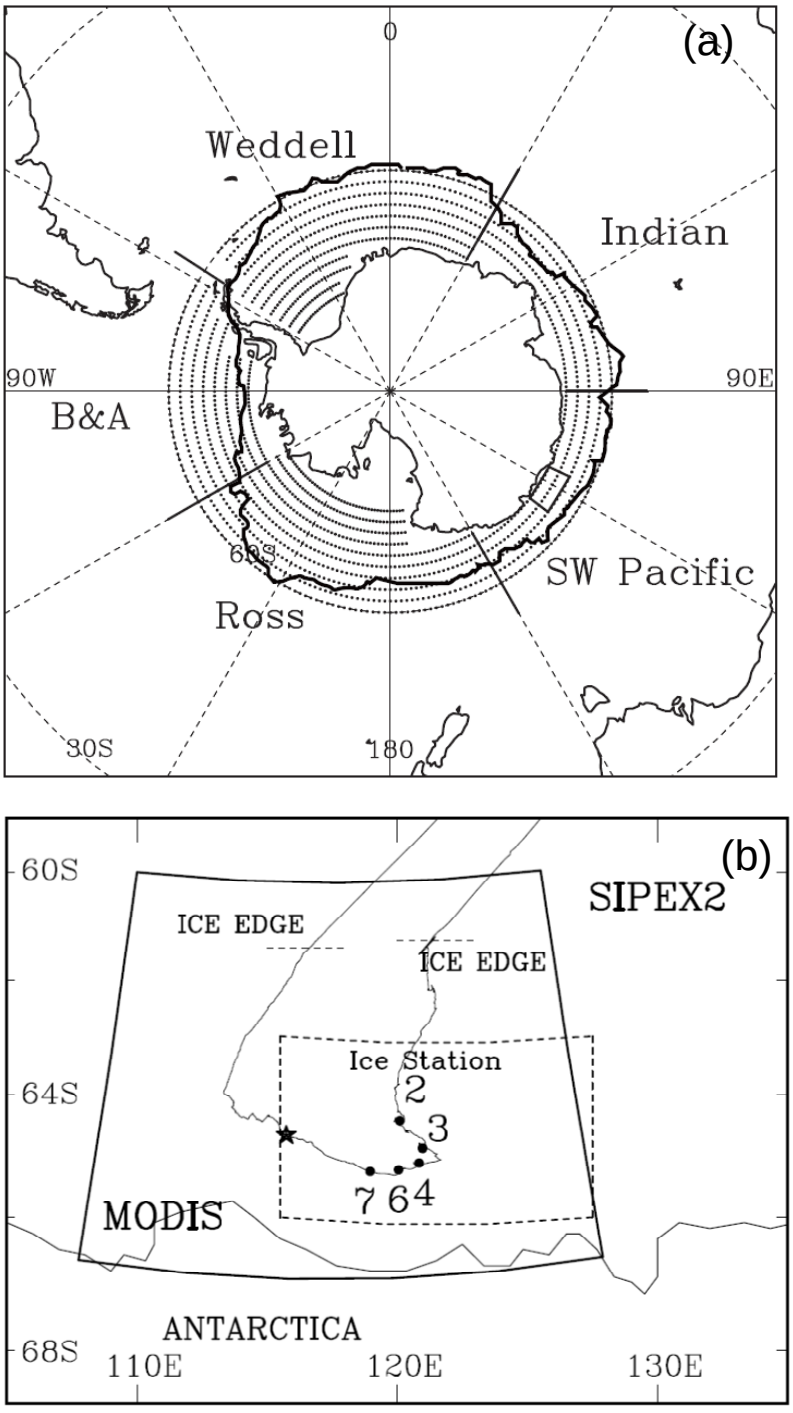
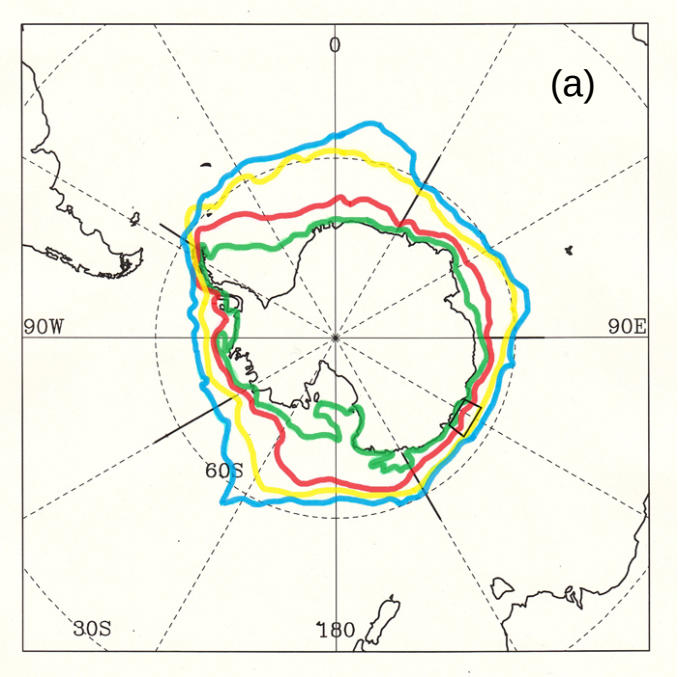

(a)
0
Weddell
Indian
90W
90E
B&A
60S
SW Pacific
Ross
30S
180
(b)
60S
SIPEX2
ICE EDGE
ICE EDGE
Ice Station
64S
2
3
7 6 4
MODIS
ANTARCTICA
68S
110E
120E
130E

Figure 1



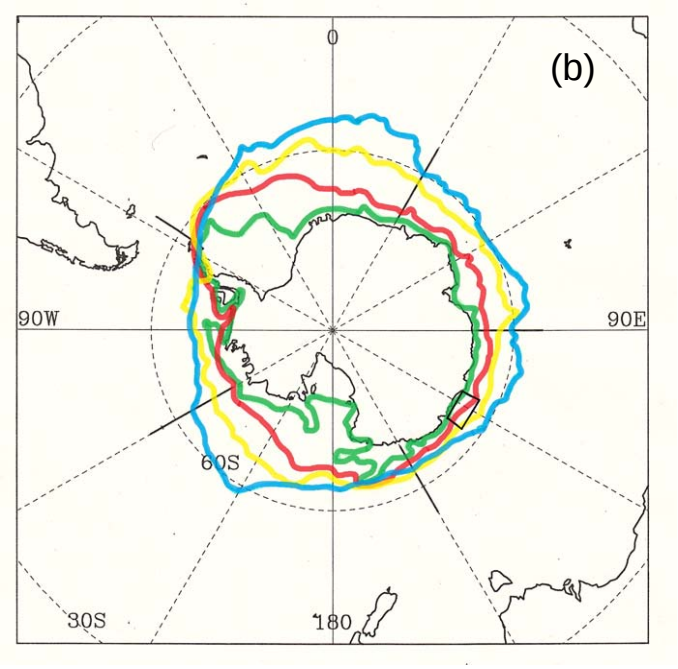


Figure 2

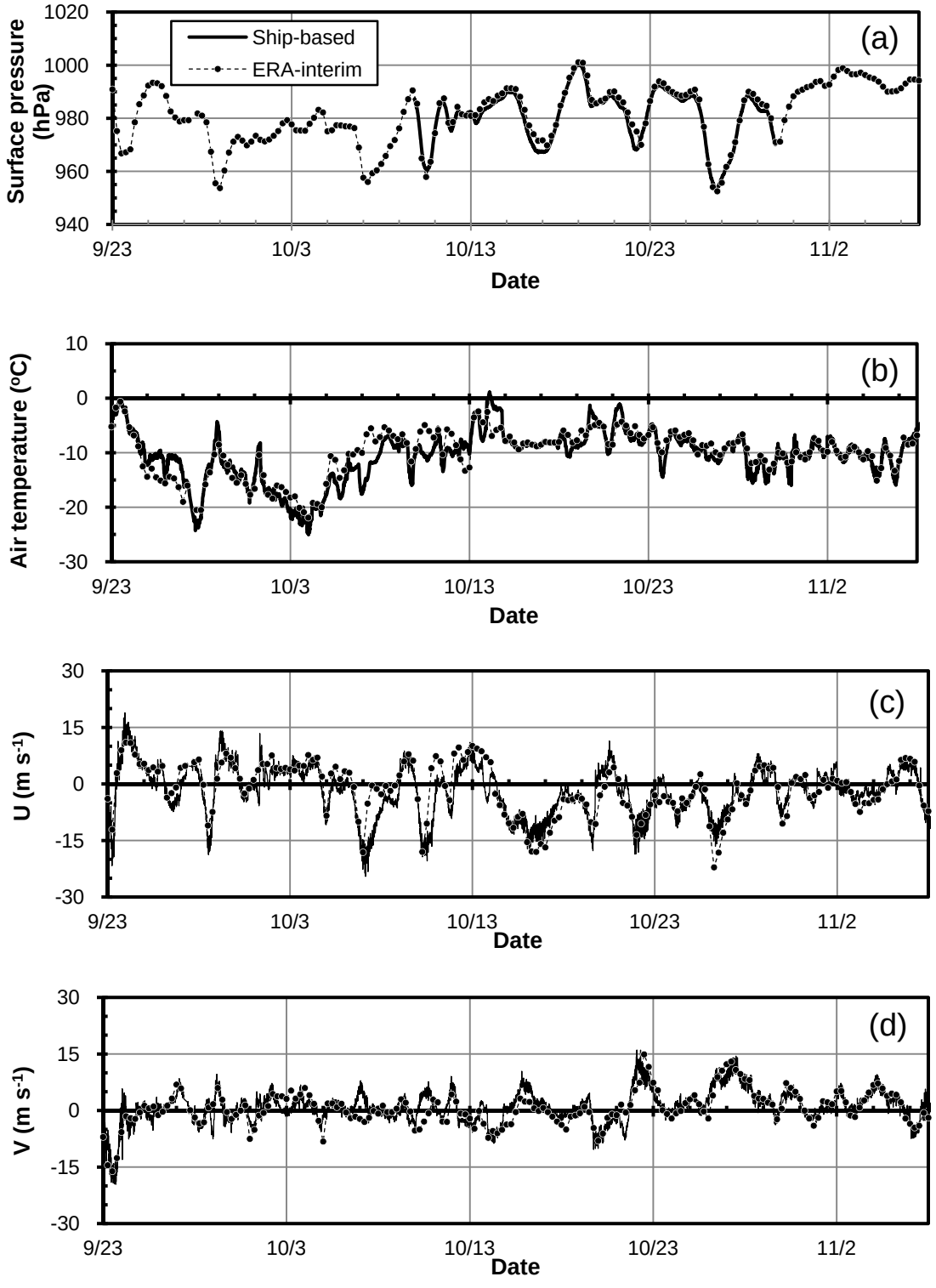

Surface pressure (hPa)
1020
1000
980
960
940
Ship-based
ERA-interim
(a)
9/23
10/3
10/13
10/23
11/2
Date
Air temperature (°C)
10
0
-10
-20
-30
(b)
9/23
10/3
10/13
10/23
11/2
Date
U (m s-1)
30
15
0
-15
-30
(c)
9/23
10/3
10/13
10/23
11/2
Date
V (m s-1)
30
15
0
-15
-30
(d)
9/23
10/3
10/13
10/23
11/2
Date

Figure 3

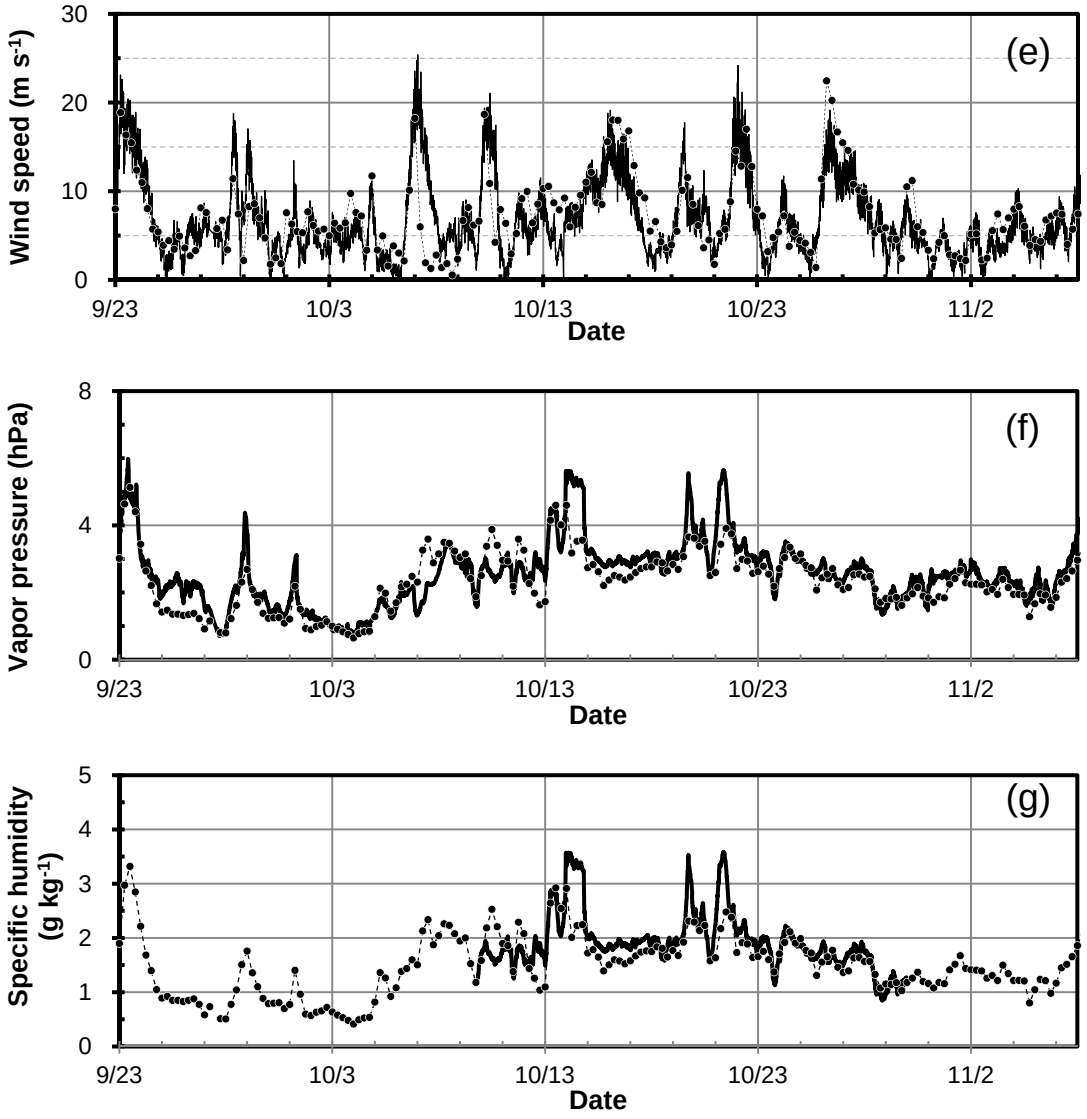
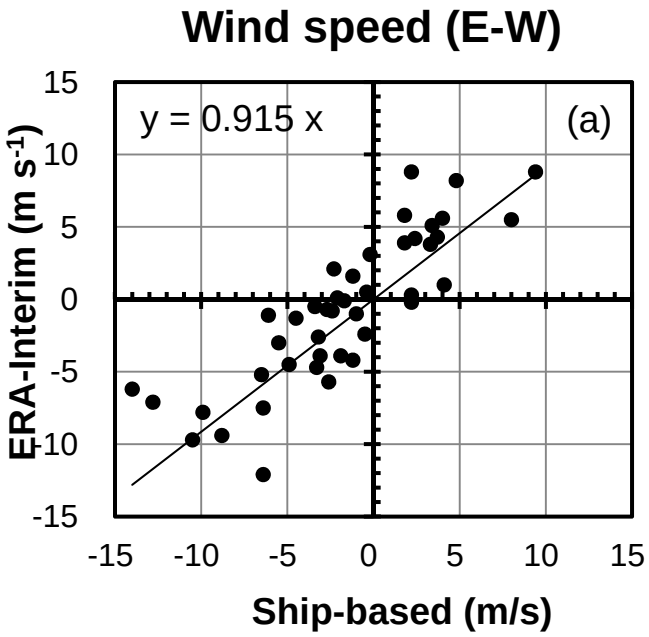


Figure 3 *(Continued)*


Wind speed (E-W)
y = 0.915 x
(a)
ERA-Interim (m s-1)
Ship-based (m/s)
15
10
5
0
-5
-10
-15
-15
-10
-5
0
5
10
15

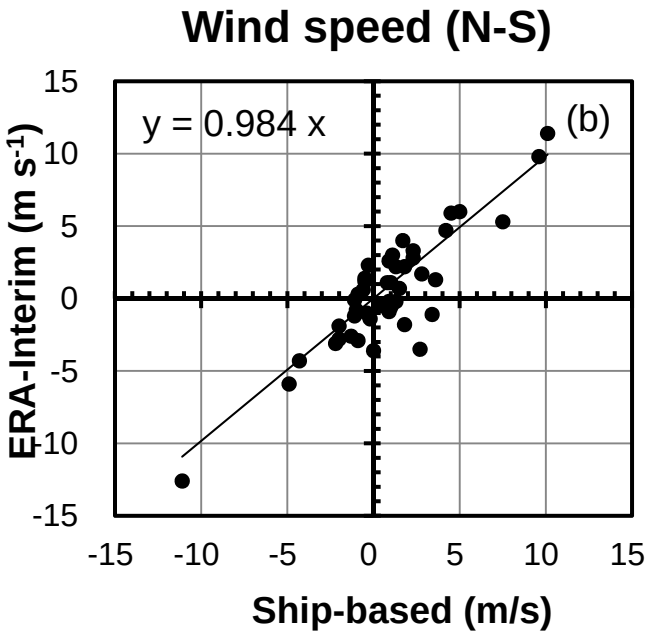

Wind speed (N-S)
y = 0.984 x
(b)
ERA-Interim (m s-1)
Ship-based (m/s)
15
10
5
0
-5
-10
-15
-15
-10
-5
0
5
10
15

Figure 4

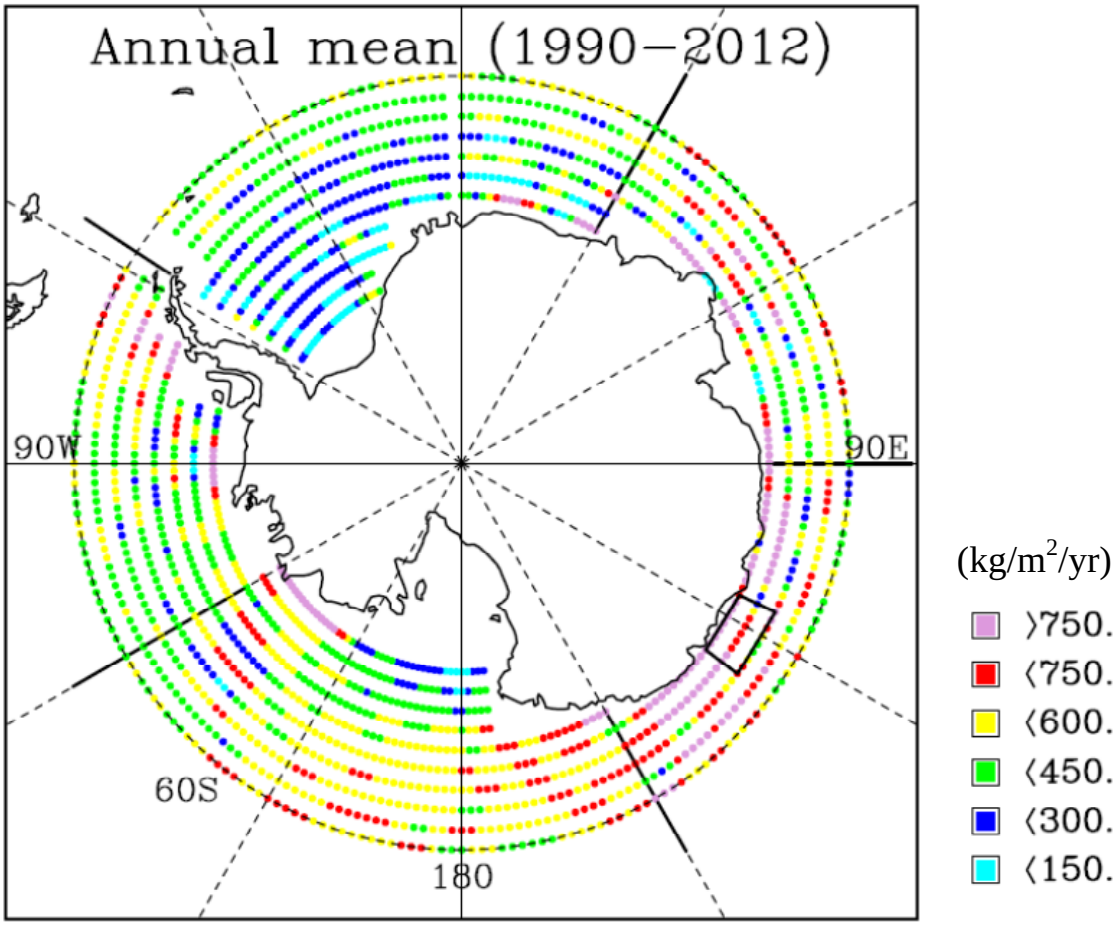
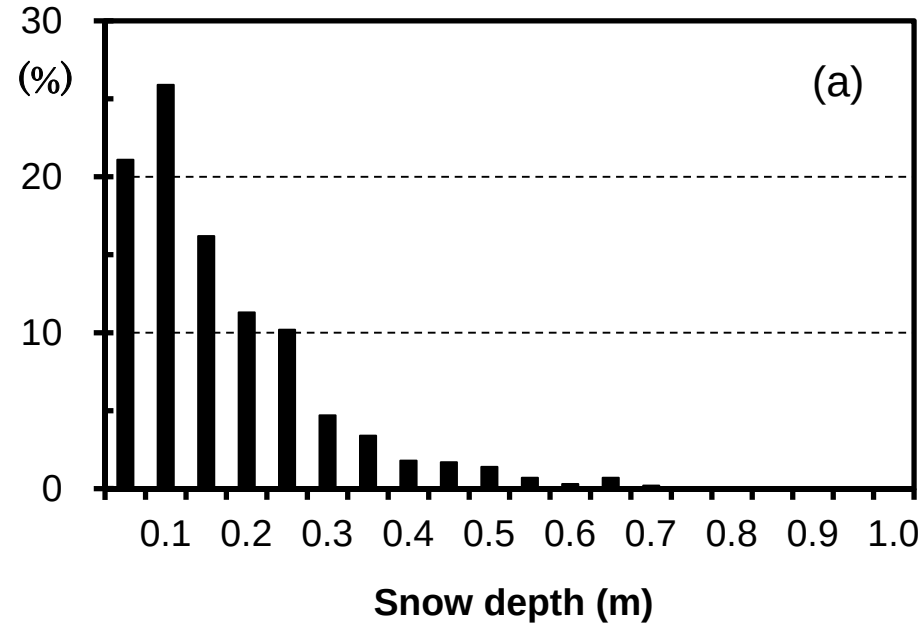

Annual mean (1990–2012)
90W
90E
60S
180
(kg/m2/yr)
〉750.
〈750.
〈600.
〈450.
〈300.
〈150.

Figure 5



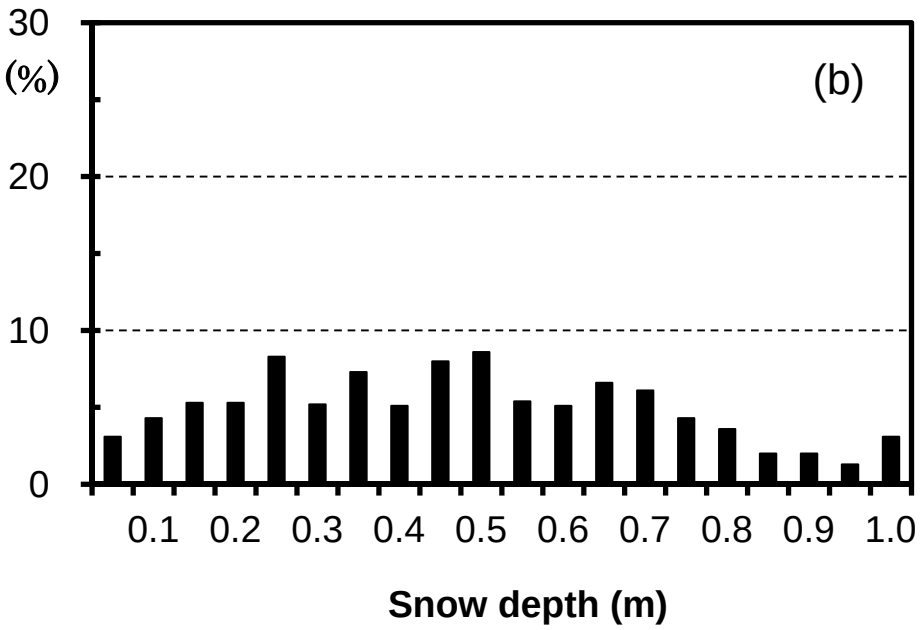


Figure 6 Histograms of snow depth.

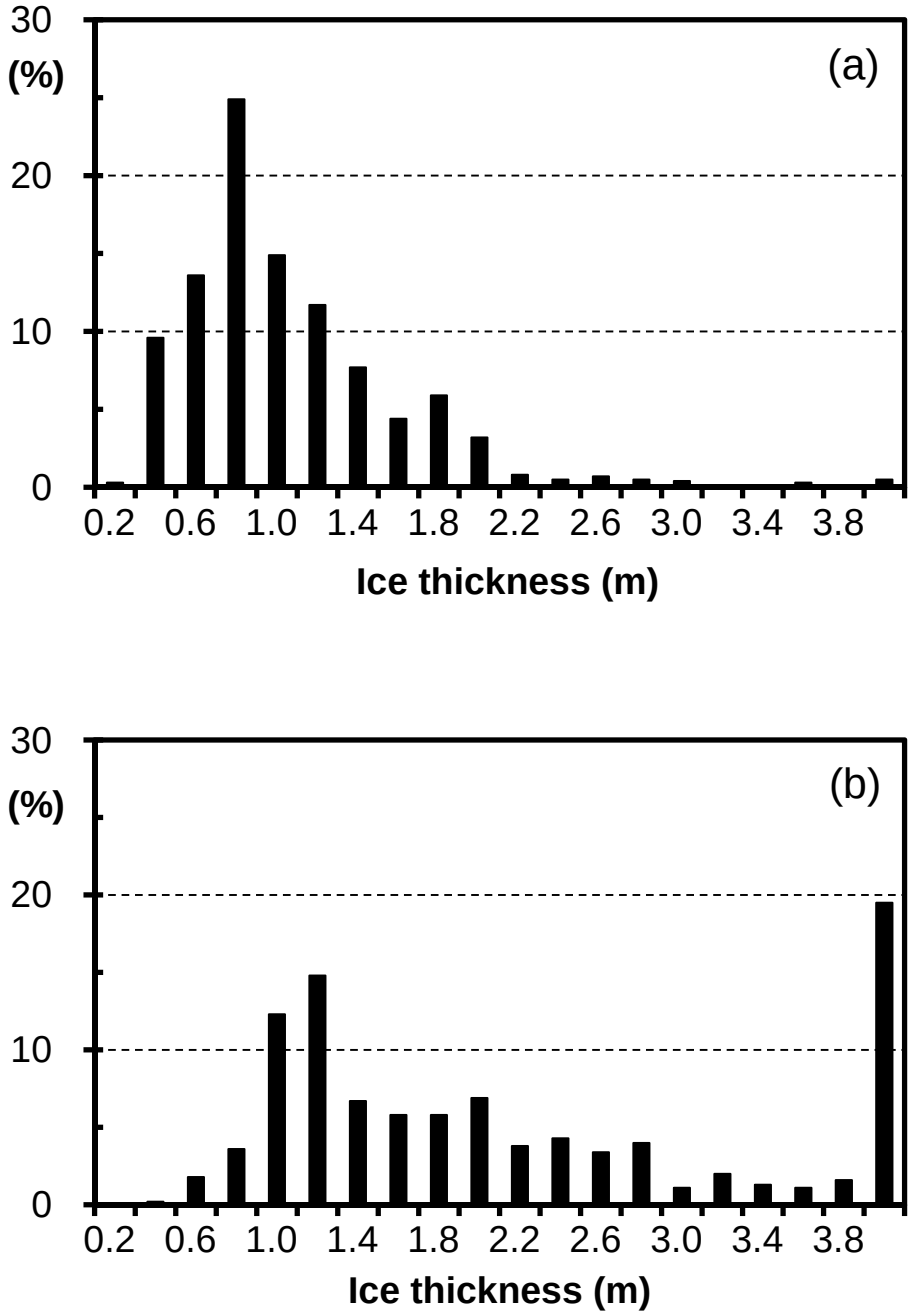


Figure 7 Histogram of ice thickness.

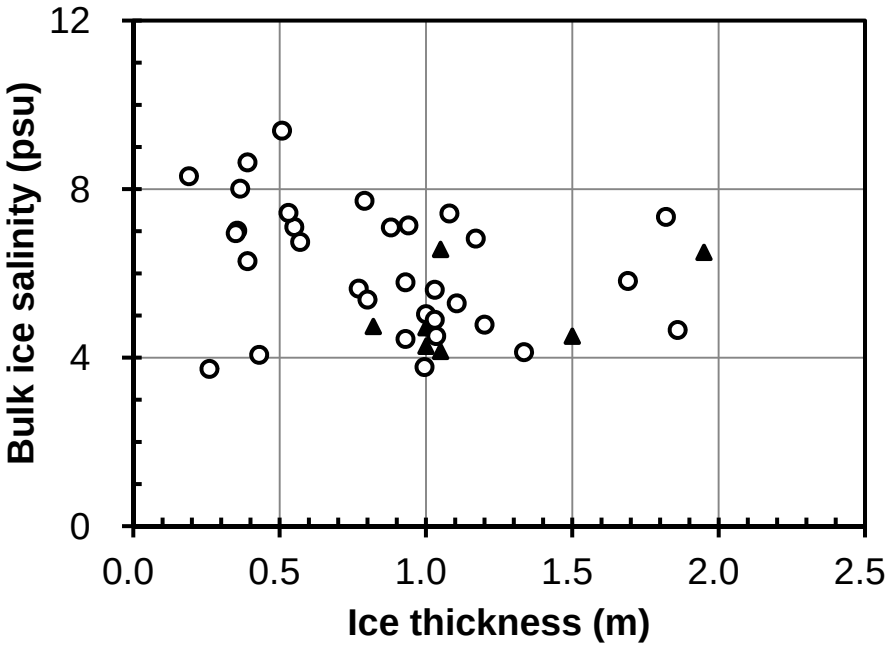


Figure 8

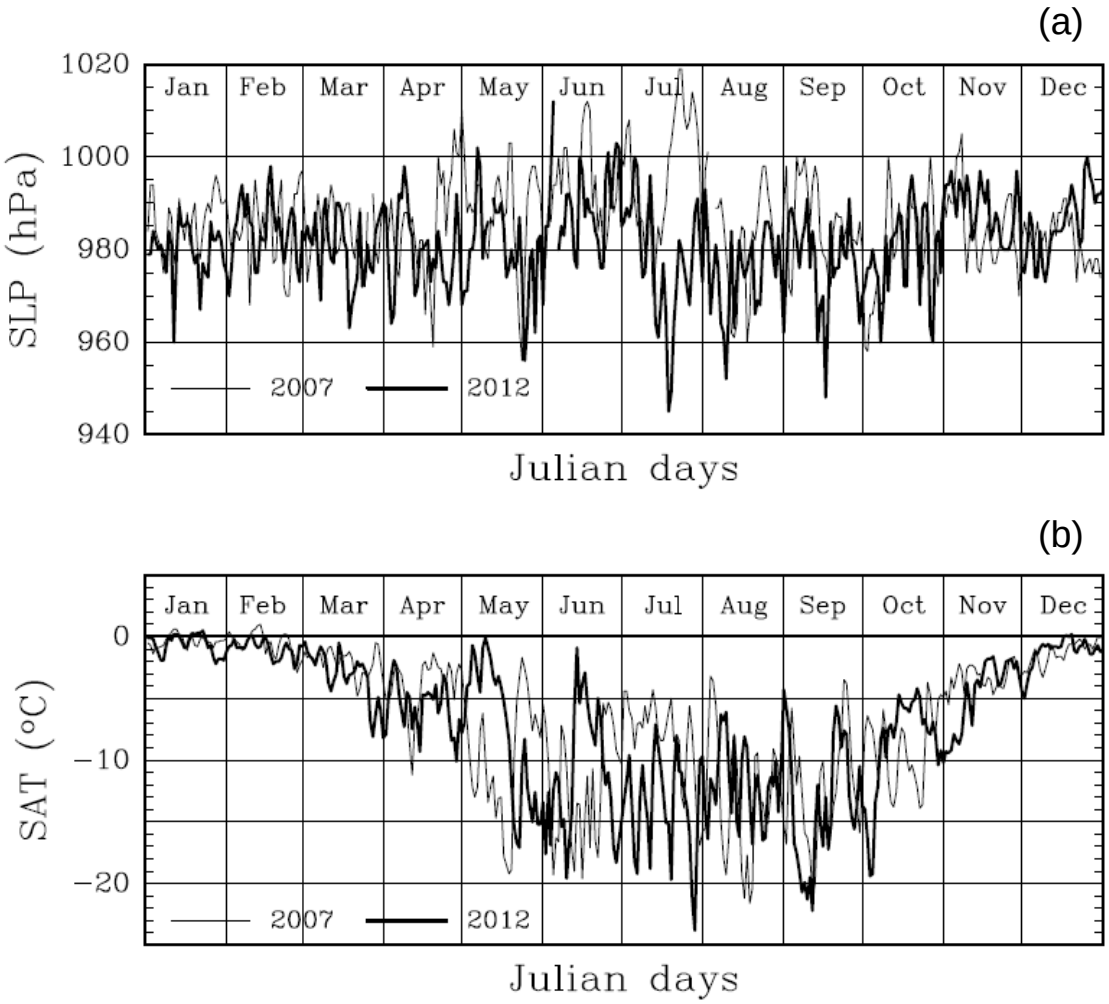

(a)
1020
1000
980
960
940
SLP (hPa)
Jan
Feb
Mar
Apr
May
Jun
Jul
Aug
Sep
Oct
Nov
Dec
2007
2012
Julian days
(b)
0
−10
−20
SAT (°C)
Jan
Feb
Mar
Apr
May
Jun
Jul
Aug
Sep
Oct
Nov
Dec
2007
2012
Julian days

Figure 9

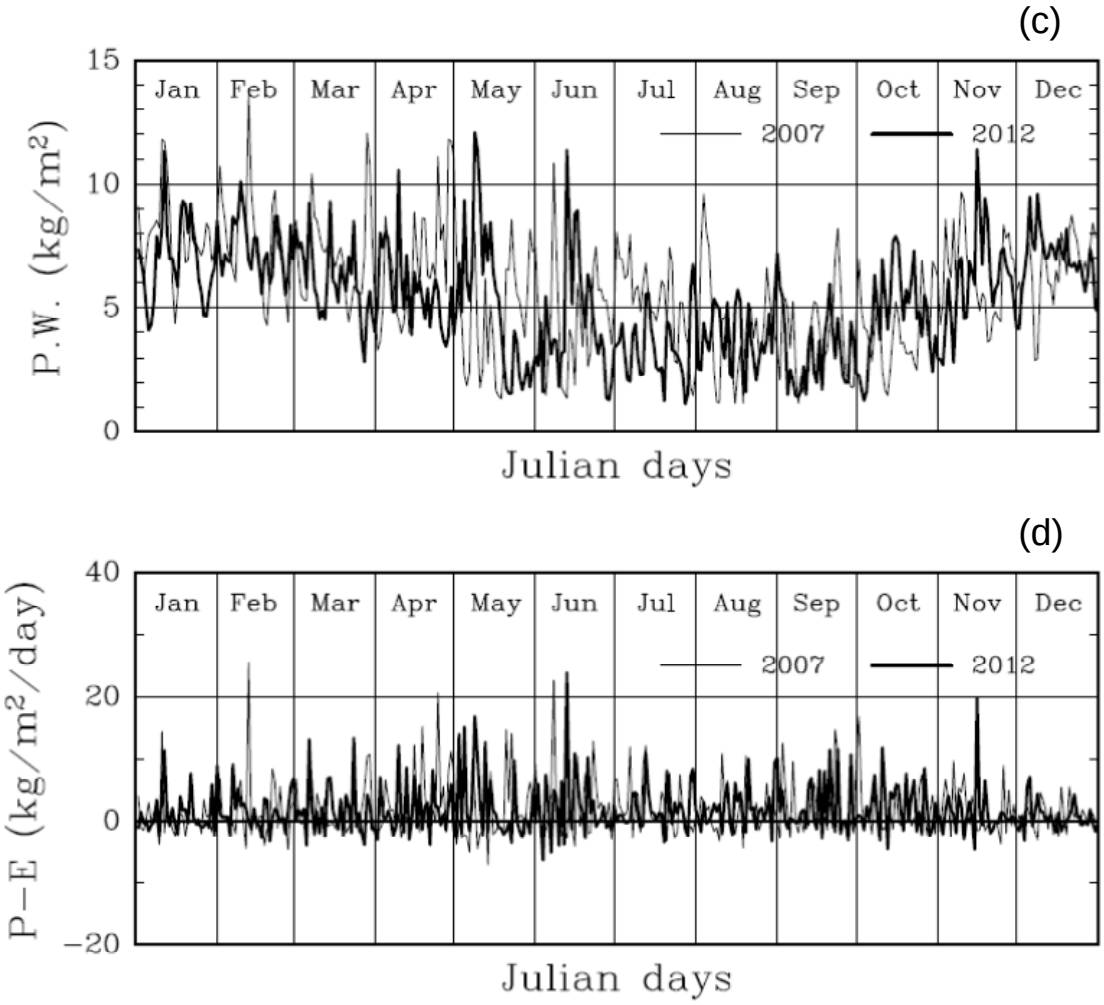
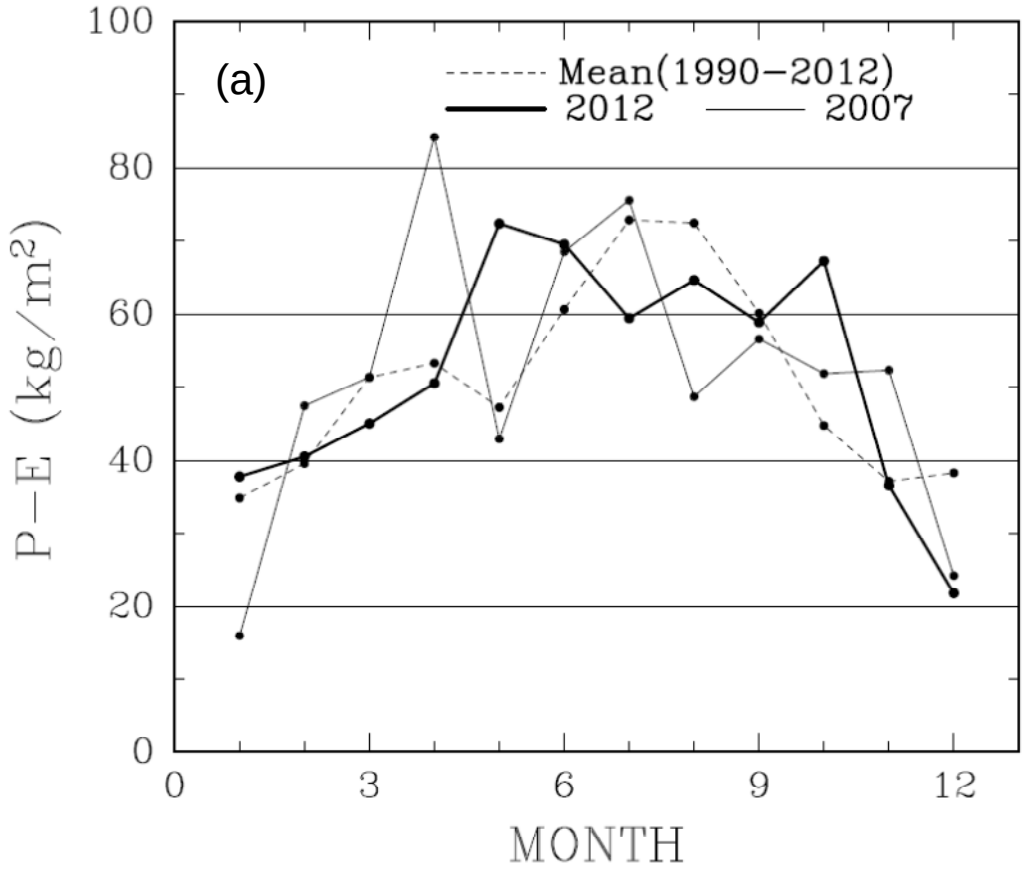


Figure 9 (*Continued.*)


(a)
Mean(1990–2012)
2012
2007
P–E (kg/m²)
MONTH
0
20
40
60
80
100
0
3
6
9
12

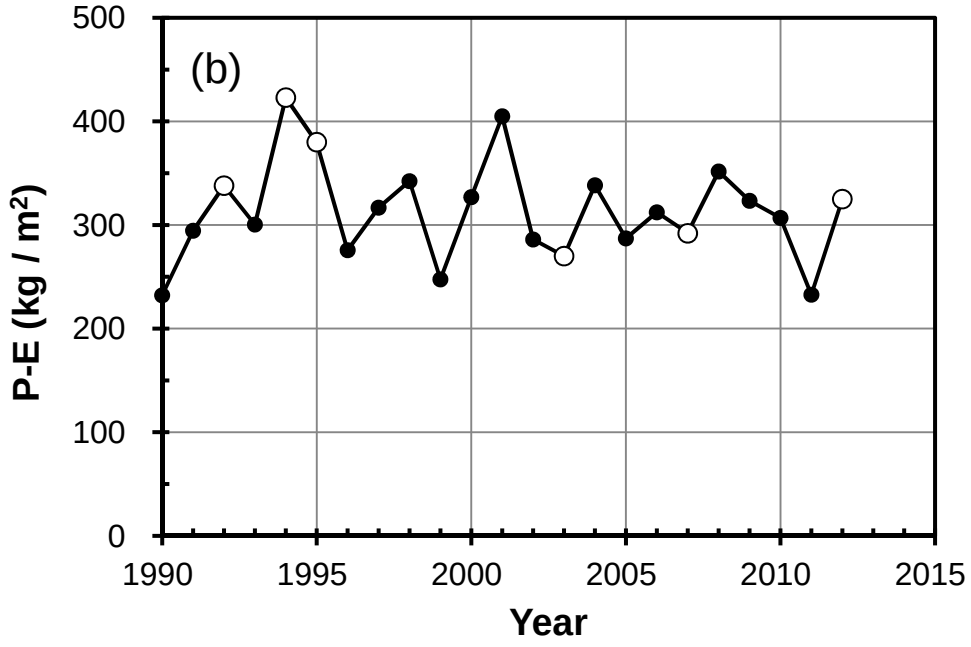

(b)
P-E (kg / m²)
Year
0
100
200
300
400
500
1990
1995
2000
2005
2010
2015

Figure 10

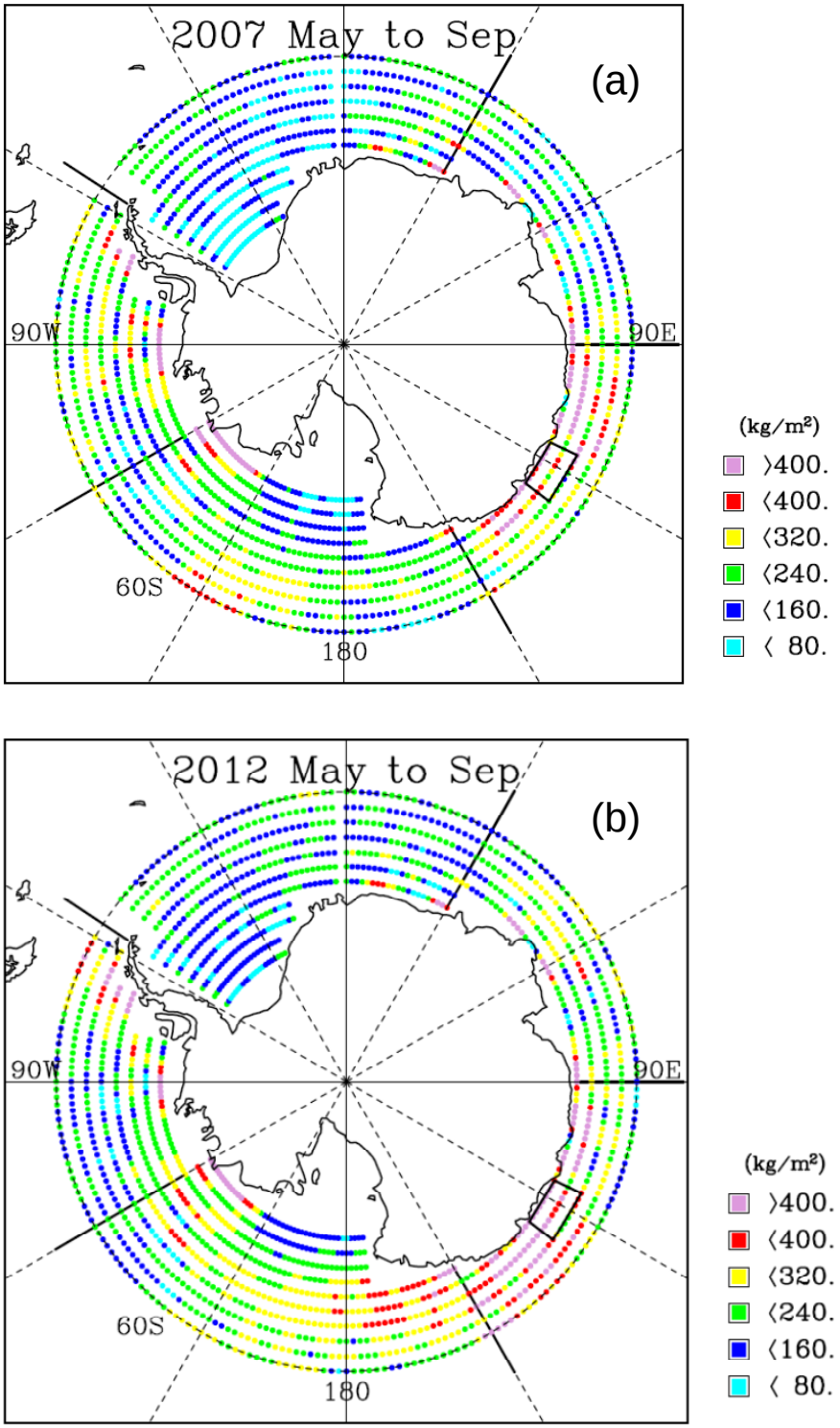

2007 May to Sep
(a)
90W
90E
60S
180
(kg/m²)
〉400.
〈400.
〈320.
〈240.
〈160.
〈 80.
2012 May to Sep
(b)
90W
90E
60S
180
(kg/m²)
〉400.
〈400.
〈320.
〈240.
〈160.
〈 80.

Figure 11

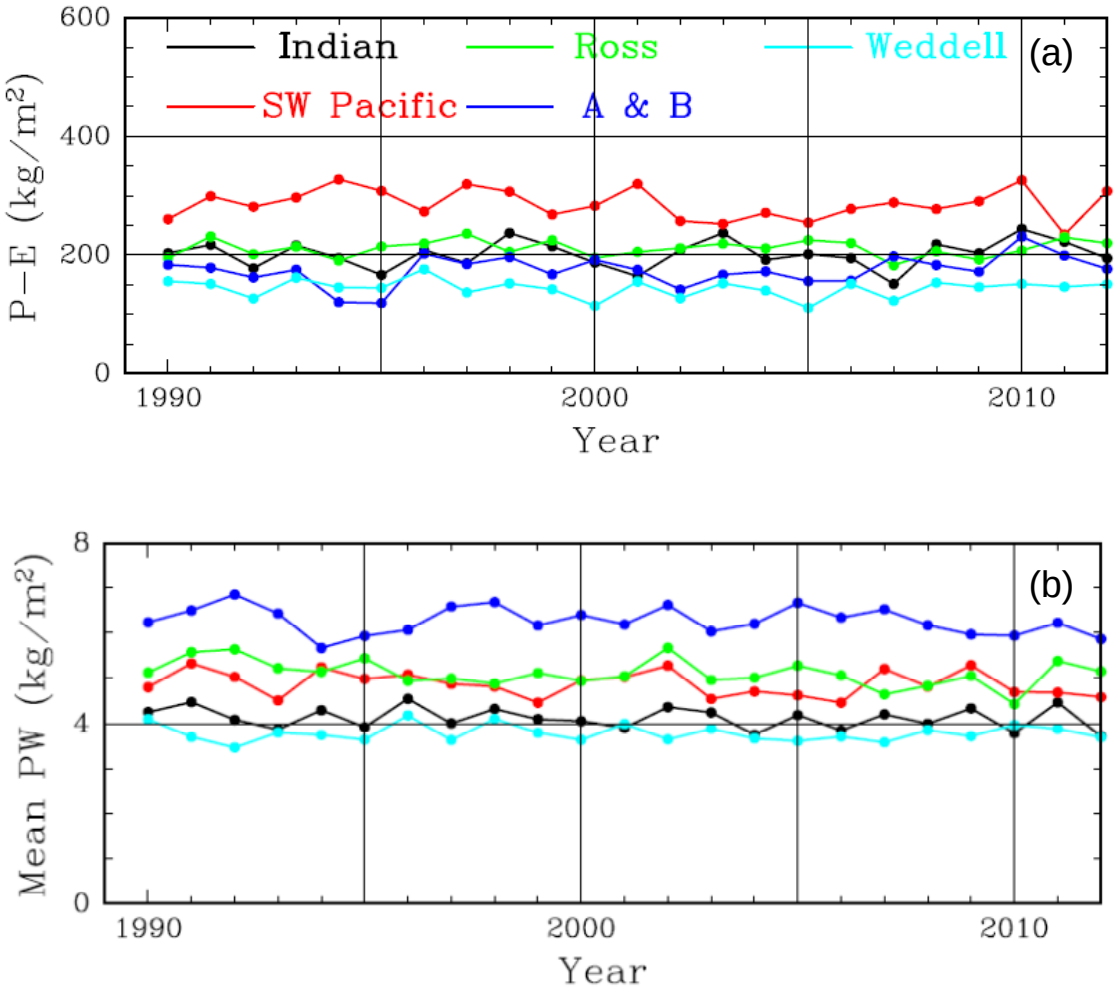

600
400
200
0
P−E (kg/m²)
Indian
Ross
Weddell
SW Pacific
A & B
(a)
1990
2000
2010
Year
8
4
0
Mean PW (kg/m²)
(b)
1990
2000
2010
Year

Figure 12

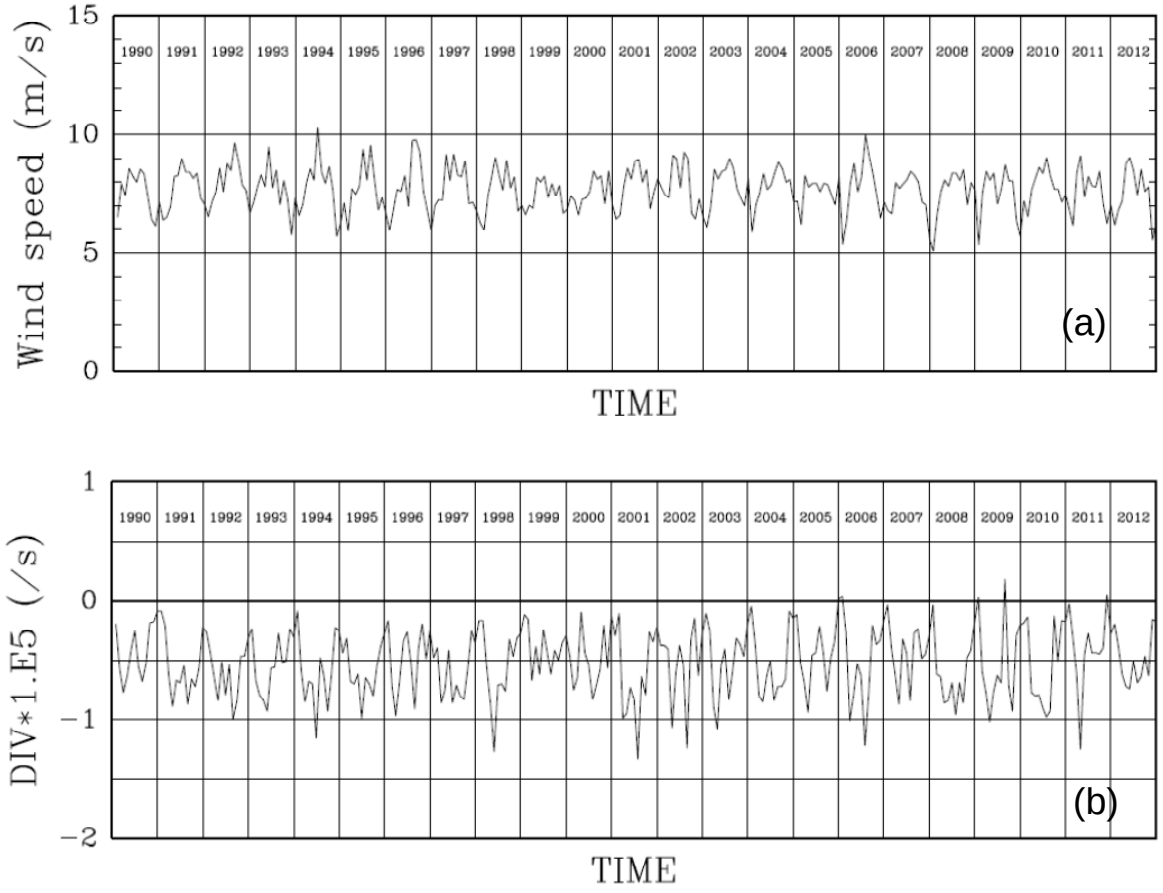

Wind speed (m/s)
15
10
5
0
1990 1991 1992 1993 1994 1995 1996 1997 1998 1999 2000 2001 2002 2003 2004 2005 2006 2007 2008 2009 2010 2011 2012
(a)
TIME
DIV*1.E5 (/s)
1
0
−1
−2
1990 1991 1992 1993 1994 1995 1996 1997 1998 1999 2000 2001 2002 2003 2004 2005 2006 2007 2008 2009 2010 2011 2012
(b)
TIME

Figure 13

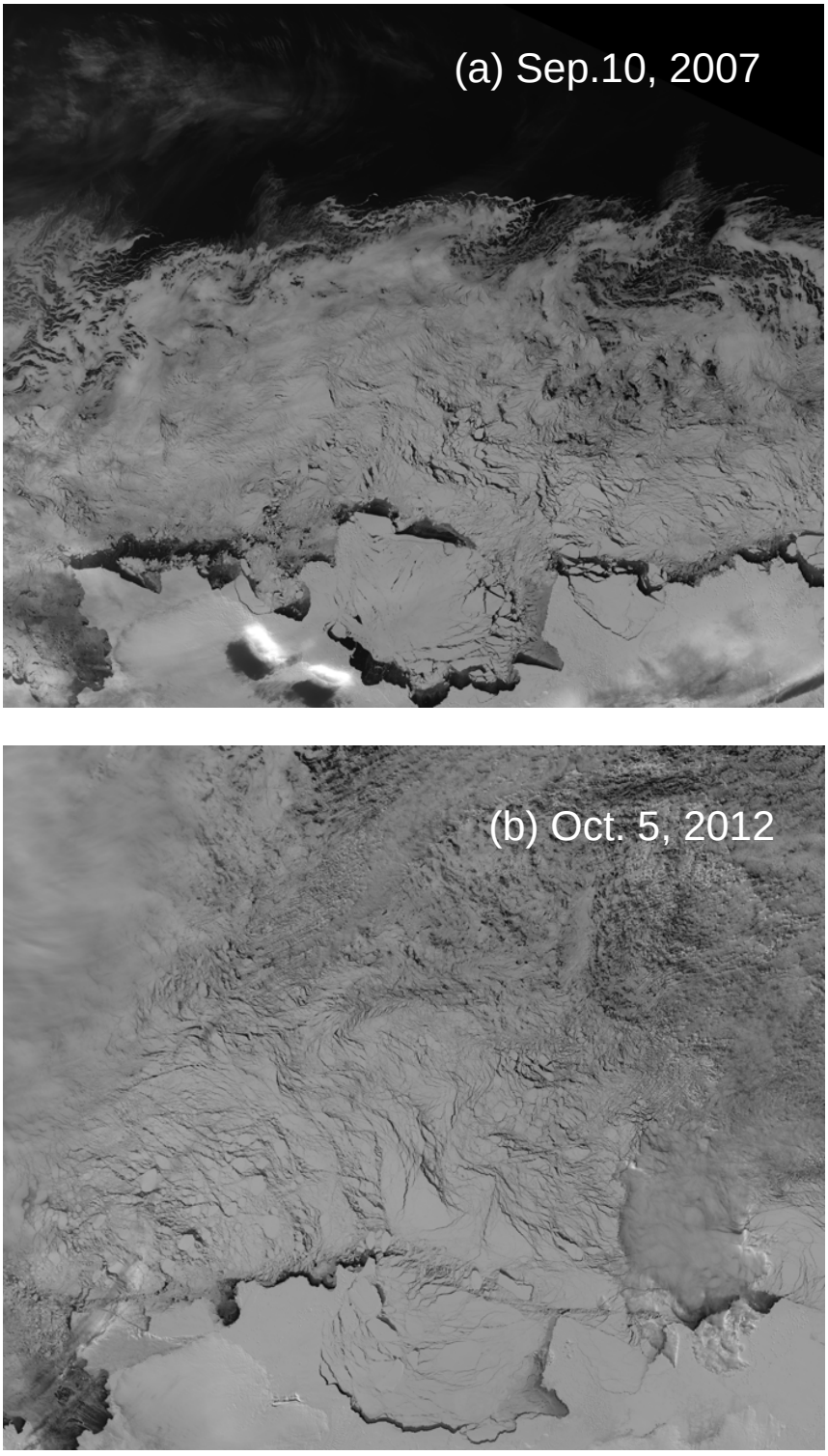


Figure 14

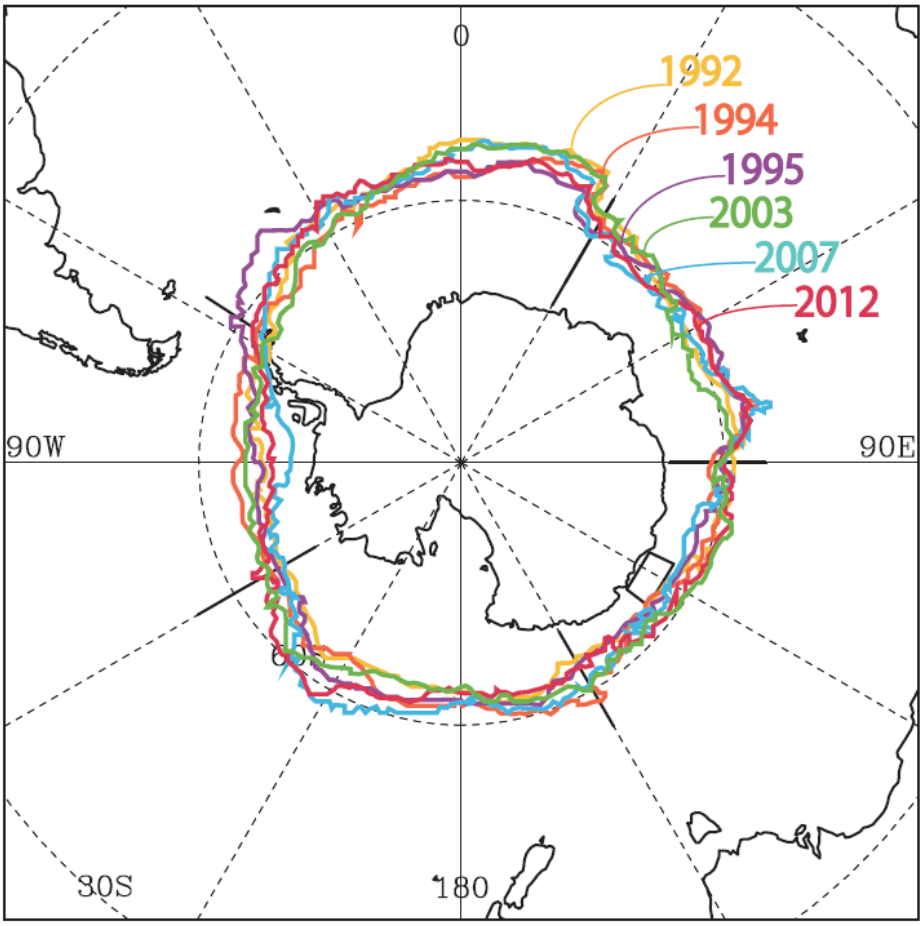


Figure 15

Table 1. The results of observation along each transect line

Transect No.	Date (2012)	Length of transect (m)	H_i (m)	F_b (m)	H_s (m)	T_i (^oC)	Snow pit number	Snow density (kg m^{-3})	Basal snow salinity (psu)
St.2-1	Sep.27-28	100	1.64	0.09	0.35	-5.1	3	350	10.2
St.2-2	Sep.27-28	100	-	-	0.31	-7.2	2	363	12.9
St.3-1	Oct. 4	100	1.79	0.12	0.55	-7.8	3	365	6.9
St.3-2	Oct. 4	100	-	-	0.47	-8.8	-	-	-
St.4	Oct. 8	100	1.37	-0.02	0.48	-4.3	3	348	12.0
St.6-1	Oct.14	100	1.73	0.10	0.28	-5.7	2	351	0.7
St.6-2	Oct.14	100	-	-	0.52	-5.2	2	332	0.5
St.7-1	Oct.20-23	100	4.87	0.29	0.52	-3.7	3	334	3.5
St.7-2	Oct.20-23	100	-	-	0.47	-4.1	-	-	-
St.7-3	Oct.20-23	100	-	-	0.56	-4.4	-	-	-
St.7-4	Oct.20-23	100	-	-	0.43	-	-	-	-
All	mean	1100	2.33	0.12	0.45	-5.8	18	350	6.8
	s.d.		1.64	0.18	0.26	3.1		46	7.0

(*) H_i: mean ice thickness, F_b: mean freeboard, H_s: mean snow depth, T_i: mean snow/ice interface temperature
Basal snow salinity means the salinity at the basal 3 cm layer of snow.
Snow density and basal snow salinity were obtained by averaging the data at all the snow pits along each transect line.
Along the transects of St.3-2, St.6-2, St.7-2, St.7-3, and St.7-4, only the snow depth measurement was conducted.
See Fig.1b for the locations of ice stations.

Table 2. Comparison with past results conducted around this region in winter

Month & Year	Longitude (E)	Snow depth (m)	Ice thickness (m)	Freeboard (m)	Mean snow density (kg/m^3)	Basal snow salinity (psu)
Oct.-Nov. 1992	62-102	0.13	-	-	-	-
Sep.-Oct. 1994	75-150	0.15	-	-	-	-
Aug. 1995	138-141	0.13	~ 0.6 (mode)	~ 0.05	360	17.0
Sep.-Oct. 2003	109-118	0.21±0.18	0.96±0.69	0.04±0.07	306	13.3
Sep.-Oct. 2007	115-130	0.14±0.13	0.98±0.58	0.07±0.10	322	13.3
Sep.-Oct. 2012	119-122	0.45±0.26	2.33±1.64	0.12±0.18	350	6.8

Table 3. Correlation coefficients between ice condition parameters

(a) 2007 (N = 11)

	Hi (Ave)	(sd)	Fb (Ave)	(sd)	Hs (Ave)	(sd)	Se (Ave)	(sd)
Hi (Ave)	1.00	0.76	0.43	**0.86**	**0.82**	**0.82**	0.78	0.67
(sd)	-	1.00	0.16	0.58	0.50	0.54	0.42	0.34
Fb (Ave)	-	-	1.00	0.76	0.37	0.41	0.76	0.78
(sd)	-	-	-	1.00	0.79	**0.80**	**0.93**	**0.88**
Hs (Ave)	-	-	-	-	1.00	**0.96**	**0.89**	**0.81**
(sd)	-	-	-	-	-	1.00	**0.88**	**0.87**
Se (Ave)	-	-	-	-	-	-	1.00	**0.96**
(sd)	-	-	-	-	-	-	-	1.00

(b) 2012 (N = 5)

	Hi (Ave)	(sd)	Fb (Ave)	(sd)	Hs (Ave)	(sd)	Se (Ave)	(sd)
Hi (Ave)	1.00	0.71	**0.92**	**0.93**	0.38	0.32	**0.91**	0.48
(sd)	-	1.00	0.67	0.73	-0.21	-0.04	0.47	0.41
Fb (Ave)	-	-	1.00	**0.99**	0.27	0.63	**0.82**	0.77
(sd)	-	-	-	1.00	0.31	0.56	**0.86**	0.76
Hs (Ave)	-	-	-	-	1.00	0.34	0.72	0.18
(sd)	-	-	-	-	-	1.00	0.43	**0.86**
Se (Ave)	-	-	-	-	-	-	1.00	0.51
(sd)	-	-	-	-	-	-	-	1.00

(*) Hi, Fb, Hs, and Se denote mean ice thickness, freeboard, snow depth, and surface elevation, respectively.
Freeboard is the height of ice surface, while surface elevation is the height of snow surface.
Values greater than 0.8 were stressed in bold letters.
Note that each parameter averaged for each transect line is used for this analysis.

Table 4. Snow volmetric balance in winter

Year	$< B >$	$< P > - < E >$	$< I >$	$< L >$
2007	0.14±0.13	0.90	0.19±0.21	0.57
2012	0.45±0.26	0.93	0.09±0.17	0.39
Difference	0.31±0.23	0.03	0.10±0.12	0.18

(*) $<B>$ denotes the spatially averaged snow accumulation rate.
$<P>-<E>$ is the spatially averaged precipitation minus sublimation.
$<I>$ denotes the snow thickness consumed for the snow ice formation.
$<L>$ denotes the snow thickness lost into leads due to snow drift.
The numbers are all in meters. The error in Difference was estimated from the difference between the two years assuming the Normal distribution.